UNIVERSITÀ DEGLI STUDI DI PADOVA

DIPARTIMENTO DI INGEGNERIA DELL'INFORMAZIONE

DEPARTMENT OF INFORMATION ENGINEERING

MASTER'S DEGREE IN BIOIENGINEERNIG OF REHABILITATION

Validation of an extended foot-ankle musculoskeletal model using in vivo 4D CT data

MASTER CANDIDATE:

Alice Bravin

SUPERVISOR:

Prof. Zimi Sawacha

Università degli studi di Padova

CO-SUPERVISOR:

Prof. Ilse Jonkers

Dr. Barbara Postolka

Dr. Bryce Killen

Katholieke Universiteit Leuven

ACADEMIC YEAR 2021/2022

Graduation date: 30.11.2022

Index

Abstract

Per simulare il movimento del corpo umano, è necessario creare dei modelli che rappresentino le strutture anatomiche. In questo elaborato ci si concentrerà su un modello biomeccanico del complesso piede-caviglia implementato in un software per la modellazione muscoloscheletrica, nella fattispecie OpenSim. OpenSim è un software che consente di sviluppare modelli di strutture muscoloscheletriche e creare simulazioni dinamiche in grado di stimare i parametri interni delle strutture anatomiche (come le forze muscolari e di contatto tra le ossa), attraverso la simulazione della cinematica e la cinetica del movimento delle varie strutture coinvolte [1].

Nel presente elaborato, si è partiti dallo studio di un dataset, acquisito da Boey et al. [2] tramite scansione 4D CT in combinazione con un dispositivo di manipolazione del piede su soggetti sani e pazienti affetti da instabilità cronica di caviglia. In questo modo è stata valutata la cinematica dell'osso del piede durante il cammino simulato.

Lo scopo di questo elaborato è quindi validare un modello del complesso piede-caviglia sviluppato da Malaquias et al. [3], partendo dai dati acquisiti affinché, imponendo il movimento della pedana, la simulazione restituisca delle variabili comparabili a quelle reali. Il modello muscoloscheletrico esteso del complesso piede-caviglia è composto da sei segmenti rigidi e cinque articolazioni anatomiche (caviglia, sottoastragalica, mediotarsica, tarsometatrsale e metatarsofalangea) per un totale di otto gradi di libertà. A questo modello è stata aggiunto una pedana (per simulare il dispositivo di manipolazione utilizzato nella sperimentazione) e sono stati incrementati i gradi di libertà delle articolazioni di caviglia e sottoastragalica, per ottenere tre gradi di libertà ciascuna. Dopodiché, è stato imposto un movimento combinato di inversione\eversione ed ab-adduzione alla pedana ed è stato valutato il movimento del modello del piede rispetto al dataset.

Abstract

To simulate the movement of the human body, it is necessary to create models that represent anatomical structures. In this thesis the focus will be placed on a biomechanical model of the complex foot-ankle implemented in a software for musculoskeletal modeling, in particular OpenSim. OpenSim is software that allows to develop models of musculoskeletal structures and create dynamic simulations capable of estimating the internal parameters of anatomical structures (such as muscle and contact forces between bones), through the simulation of the kinematics and kinetics of the movement of the various anatomical structures involved [1].

In this paper, the starting point was the study of a dataset, acquired by Boey et al. [2] with 4D CT scan in combination with a foot manipulator device. The study was run on healthy subjects as well as patients with chronic ankle instability. In this way, the kinematics of the movement of the foot bones during simulated gait was evaluated.

The aim of this project was to validate a model of the foot-ankle complex, developed by Malaquias et al. [3], starting from the acquired data, so that, by imposing the movement of the platform, the simulation would return variables comparable to the dataset. This extended musculoskeletal model of the foot-ankle complex is composed of six rigid segments and five anatomical joints (ankle, subtalar, midtarsal, tarsometatarsal, and metatarsophalangeal) for a total of eight degrees of freedom. A footplate was added to this model (to simulate the foot manipulator device utilized in the experiment) and the degrees of freedom of the ankle and subtalar joints were increased, to obtain three degrees of freedom each.

After that, a combined inversion\eversion and plantar\dorsiflexion movement was imposed on the footplate and the movement of the foot model was evaluated against the dataset.

Introduction

Studying human motion is crucial for physical therapy, medicine, sports, neuroscience, and prosthesis implantation. It can be used to better understand motion-related pathologies, as a diagnostic tool, or to assist pre and post surgeries patients. Some of the data that can be obtained and studied might be joint kinematics, movement of anatomic segments, and muscle forces and length.

It is possible to observe human motion with so-called motion capture technologies, however when it comes to measuring joint and muscle reaction forces, motion capture fails to provide detailed data. The electric activity of muscles can be measured with Electromyography (EMG), but it has been demonstrated that it has a nonlinear connection with muscle forces [4].

For this reason, musculoskeletal models are largely used in motion analysis. They consist of a mechanical representation of bones, muscles, tendons, and joints and can be used to estimate measurements that can be difficult or impossible to acquire with non-invasive procedures (i.e., muscle forces or stretch and recoil of tendons). The models are used to simulate different types of movements, like walking, jumping, squatting, and more.

The body of interest (it can also be the whole human body) is modelled as a series of rigid segments linked by joints and activated by muscles. Musculoskeletal models can be used to study many types of movement and can have as few or as many body segments as needed to answer the issue addressed. For example, the model used to simulate walking minimally includes segments from the pelvis as well as both legs and feet. These segments can represent just one bone or incorporate many. The more segments the model has, the more detailed the movement analysis can be.

The results of musculoskeletal simulations are used in direct application processes, such as diagnostic and surgical planning or in product design. Therefore, it is important that models are accurate in their predictions, otherwise they can develop erroneous output. To assure that a model's output is correct, it needs to go through a process called *validation*. This process determines how well the model represents the real word and experimental data, and it does it by comparing the model to real experimental results (this can be from motion capture or medical imaging) [5].

OpenSim [6] is one of many software that can be used to develop musculoskeletal models and conduct dynamic simulation of movement.

In this paper the focus will be placed on a OpenSim foot musculoskeletal model. The foot is a complex structure and models can often oversimplify its anatomy, not allowing it to evaluate detailed foot motion.

Chapter 1

1. Foot biomechanics

This chapter will give a brief explanation of the anatomy and biomechanics of the foot, in order to better understand the terminology that will be used later in the thesis.

1.1 Foot anatomy

The foot is a complex anatomical and biomechanical structure, placed at the distal end of each lower limb of the human body. It is composed of 26 bones, 33 joints and a hundred of muscles, tendons, and ligaments [7]. The position and name of the foot bones are described in figure 1.1.
The function of the foot is to transmit force between the lower limb and the ground, providing support and balance during standing and stabilizing the body during gait. [7]

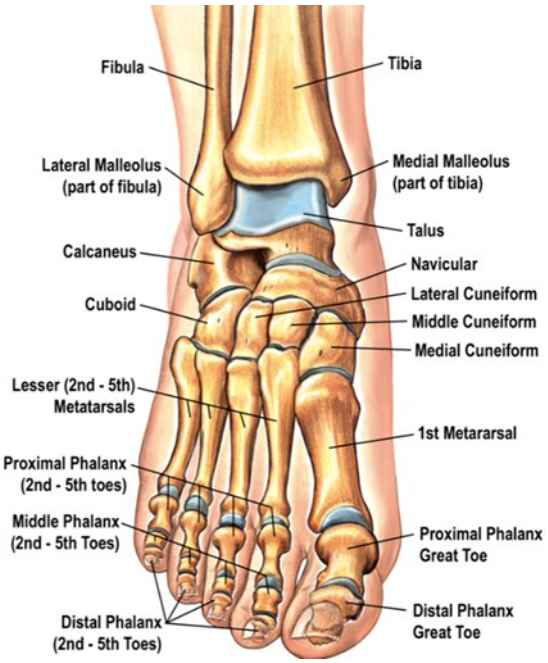

Figure 1.1: Bones of the foot [8].

The most important anatomical structures of the foot are:

- The bony skeleton, which, along with ligaments and arches, offer relative rigidity and provides the lever arm mechanism needed to support propulsion and maintain balance while standing.
- The joints that provide flexibility.
- The tendons and muscles that regulate foot movement. [8]

1.1.1 Foot joints and ligaments

Foot joints allow the movement of the foot, which is essential for human motion (such as walking, jumping, etc.). The ligaments are made of fibrous connective tissue and fulfil the function of connecting bones to other bones [9].

Ankle joint:

The ankle joint (or talocrural joint) is a hinge joint that involves the talus of the foot and tibia (forming the tibiotalar joint) and fibula (forming the fibulatalar joint) of the leg (figure 1.2). Is uniaxial and allows plantar/dorsiflexion. The muscle that allows dorsiflexion is the *tibialis anterior,* while the *soleus* and *gastrocnemius* muscles allow plantar flexion.

The joint gains its stability from bony congruence, a fibrous capsule, and the ligaments support.

The ligaments, that stabilize the ankle, are:

- *Medial collateral ligament*: it is a triangular band, commonly called *deltoid ligament*, that connects proximally to the medial malleolus and distally to calcaneus, talus, and navicular bones. There are four major fibre groups in the ligament: tibionavicular fibres (anterior segment), tibiocalcaneal fibres (intermediate segment), anterior tibiotalar fibres (deep segment) and posterior tibiotalar fibres (posterior segment).
- *Lateral collateral ligament*: it is formed of three separate ligaments: anterior talofibular ligament (that connects the talus to the lateral malleolus of the fibula), posterior talofibular ligament (that travels horizontally from the distal part of the fibular malleolus to the posterior process of the talus), and the calcaneofibular ligament (that travels from the fibular malleolus to the calcaneus). [10]

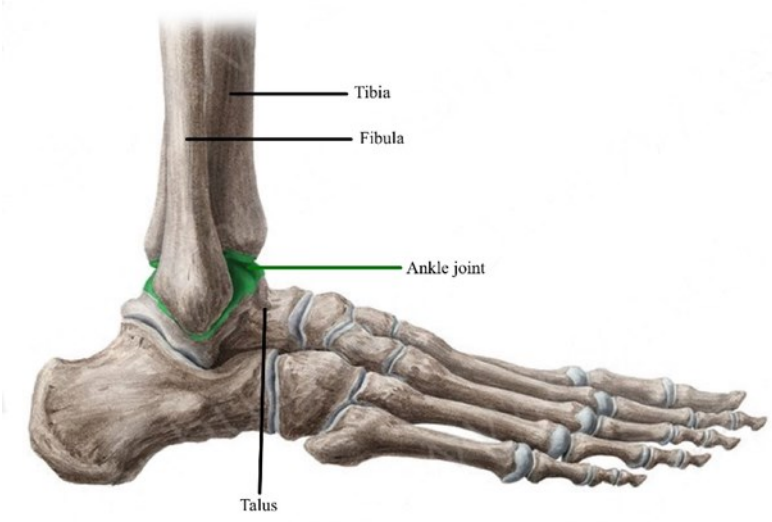

Figure 1.2: Ankle joint [10].

Subtalar joint:

The subtalar joint consists of two separate joint cavities: an anterior and a posterior articulation. The anterior articulation, which involves the talar head, anterior-superior facets, sustentaculum tali (a horizontal eminence on the calcaneus) and the concave surface of the navicular. Is referred to as the talocalcaneonavicular joint, and functions as a ball and socket, this joint is represented in the figure 1.3. The posterior articulation, known as talocalcaneal joint, involves the inferior-posterior talar facet and the superior-posterior facet of the calcaneus. Is shown in figure 1.4B [7].

The two joints have separate joint capsules, divided by the *sinus tarsi*.

The talocalcaneonavicular joint is stabilized by a fibrous capsule and two ligaments:

- *Talonavicular ligament*: a thin band connecting the dorsal aspect of the talar neck with the navicular bone.
- *Plantar calcaneonavicular ligament* (spring ligament): connects the anterior aspect of the sustentaculum tali to the plantar surface of the navicular bone.

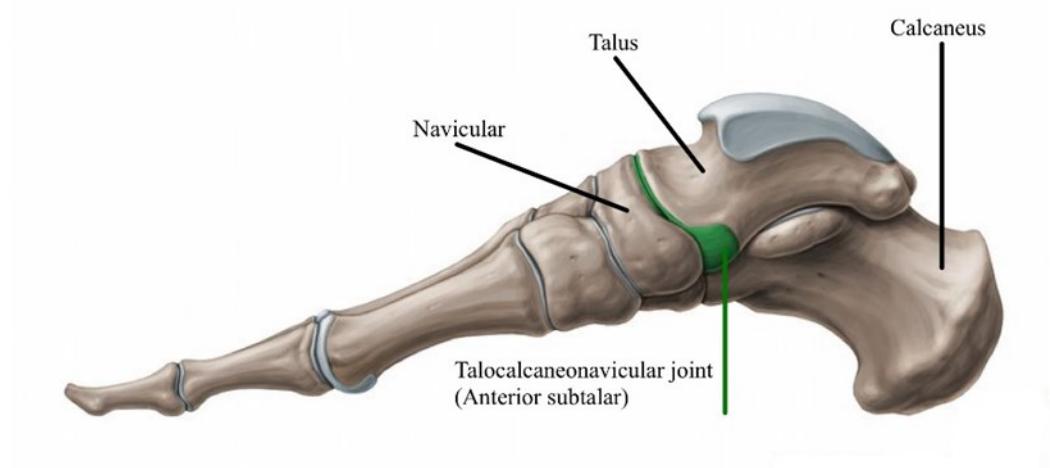

Figure 1.3: Talocalcaneonavicular joint [10].

The talocalcaneal joint is stabilized by a fibrous capsule and four ligaments:

- *Medial talocalcaneal ligament*: connects the medial tubercle of the talus with the sustentaculum tali.
- *Lateral talocalcaneal ligament*: connects the lateral process of the talus with the lateral aspect of the calcaneus.
- *Interosseus talocalcaneal ligament*: runs between the sulcus tali (a groove on the inferior aspect of the talus) and the calcaneus sulcus.
- *Cervical ligament*: connects the superior calcaneal surface to the inferior-lateral tubercle on the talar neck.

The subtalar joint allows inversion-eversion. The muscles that allow heel inversion are *tibialis anterior*, *tibialis posterior*, *gastrocnemius,* and *soleus*; the heel eversion is the result from the action of *fibularis longus*, *fibularis tertius,* and *fibularis brevis* muscles. [10]

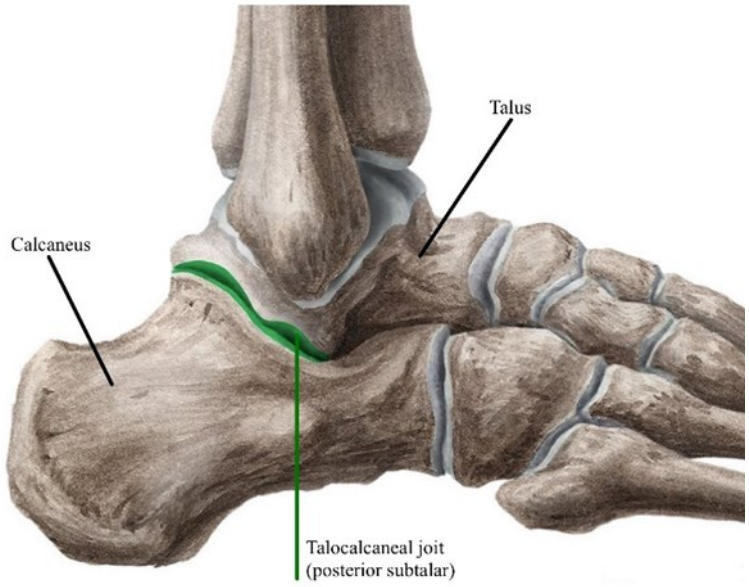

Figure 1.4: Talocalcaneal joint [10].

Calcaneocuboid joint:

The calcaneocuboid joint is a saddle (biaxial) joint and is formed by the distal surface of the calcaneus and the proximal aspect of the cuboid.

The muscles that produce this joint movement are the same as the subtalar joint: *tibialis anterior*, *tibialis posterior*, *gastrocnemius,* and *soleus* that allow inversion, and *fibularis longus*, *fibularis tertius,* and *fibularis brevis* muscles that allows eversion. These muscles allow the gliding and rotational movements between calcaneus and cuboid bones.

The ligaments that stabilize the calcaneocuboid joint are:

- *Bifurcate ligament*: a Y-shaped band that connects the anterior aspect of the calcaneus with the dorsomedial surface of the cuboid and the dorsolateral aspect of the navicular.
- *Long plantar ligament*: runs from the plantar surface of the calcaneus to the tuberosity located on the plantar aspect of the cuboid.
- *Plantar calcaneocuboid ligament*: runs from the anterior tubercle of the calcaneus to the plantar aspect of the cuboid. [10]

Naviculocuneiform joint:

The naviculocuneiform joint is a compound joint and consists of articulations between the navicular and the three cuneiform bones.

Slight gliding and rotation occur at this joint. The muscles that produce these movements are: *fibularis longus* and *brevis, tibialis anterior* and *tibialis posterior*.

The ligaments that help connecting the bones of the joint are:

- *Dorsal* and *plantar ligament*: connect the navicular bone with each cuneiform.
- *Medial dorsal ligament*: act as a capsule around the medial aspect of the joint.

Cuboideonavicular joint:

The cuboideonavicular joint is a syndesmosis that connects the cuboid and navicular bones.

This joint is stabilized by *dorsal, plantar* and *interosseous ligaments*.

The movement of this joint is produced by the same muscles of the naviculocuneiform joint.

Intercuneiform and cuneocuboid joints:

The intercuneiform and cuneocuboid joints are synovial joints involving the cuneiform and cuboid bones.

The bones are connected by:

- *Dorsal and plantar ligaments*: consist of three transverse bands, which connects the cuneiform bones and the lateral cuneiform with the cuboid.
- *Interosseous ligaments*: connect non-articular surfaces of the bones.

The movement of these joints is produced by the same muscles of the naviculocuneiform joint.

Tarsometatarsal joints:

The tarsometatarsal joints connect the metatarsal with the tarsal bones. The first metatarsal forms an articulation with the medial cuneiform, the second with the intermediate cuneiform and the third with the lateral cuneiform. The lateral cuneiform also articulates with the fourth metatarsal. Lastly, the cuboid bone articulates with both the fourth and fifth metatarsal. These joints are highlighted in pink in figure 1.5.

These joints allow flexion and extension movements of the toes; in particular the muscles that allow these movements are the *short* and *long extensors* and *flexors of the toe*.

Also, the first tarsometatarsal joint allows abduction and rotation. These movements are carried out by the *tibialis anterior* and *fibularis longus muscles*.

The ligaments involved in stabilising the tarsometatarsal joints are divided in three bands:

- *Dorsal tarsometatarsal ligaments*: there are eight and connect the metatarsal bones to the cuboid and cuneiform bones. These ligaments connect: the first metatarsal with the medial cuneiform, the second metatarsal to each cuneiform, the third metatarsal to the lateral

cuneiform, the fourth metatarsal to the lateral cuneiform and cuboid, the fifth metatarsal to the cuboid.

- *Plantar tarsometatarsal ligaments*: consist of both longitudinal and oblique bands.
- *Interosseus cuneometatarsal ligaments*: there are three. The Lisfranc's ligament runs from the second metatarsal to the lateral aspect of the medial cuneiform, the other two ligaments connect the lateral cuneiform with the base of the fourth metatarsal.

Intermetatarsal joints:

The intermetatarsal joints are formed between the metatarsal bones. These joints are stabilized by *intermetatarsal interosseous ligaments* and *dorsal* and *plantar intermetatarsal ligaments*.

Metatarsophalangeal joints:

The metatarsophalangeal joints are ellipsoid joints, which connect the heads of the metatarsals and the bases of the proximal phalanges, these joints are represented in green in figure 1.5. These articulations allow movements of flexion and extension and abduction and adduction. The muscles that produce flexion are *flexor digitorum brevis, lumbricals* and *interossei* for the lateral four metatarsophalangeal joints, and *flexor hallucis longus* and *brevis* for the hallux.

The extension is produced by the *extensor digitorum longus* and *brevis* and the *extensor hallucis longus*.

Abduction is produced by the *adductor hallucis* and the *plantar interossei*, whilst adduction is produced by the *abductor hallucis*, the *dorsal interossei* and the *abductor digiti minimi*.

The ligaments that stabilize these ligaments are the *intersesamoid ligament* (that connect together the sesamoid bones), *the plantar ligaments, the deep transverse metatarsal ligaments* and *the collateral ligament*s.

Interphalangeal joints:

The interphalangeal joints connect the trochlear surface of the phalangeal heads with the curved surface of the bases of the corresponding phalanges, these can be seen coloured in blue in figure 1.5. These hinge joints are stabilized by an articular capsule and two *collateral ligaments*.

In these joints, flexion and extension are the possible motions. The muscles that produce flexion are the *flexor digitorum longus* and *brevis* and the *flexor hallucis*. The muscles that produce extension are the *extensor digitorum longus* and brevis and *extensor hallucis longus.* [10]

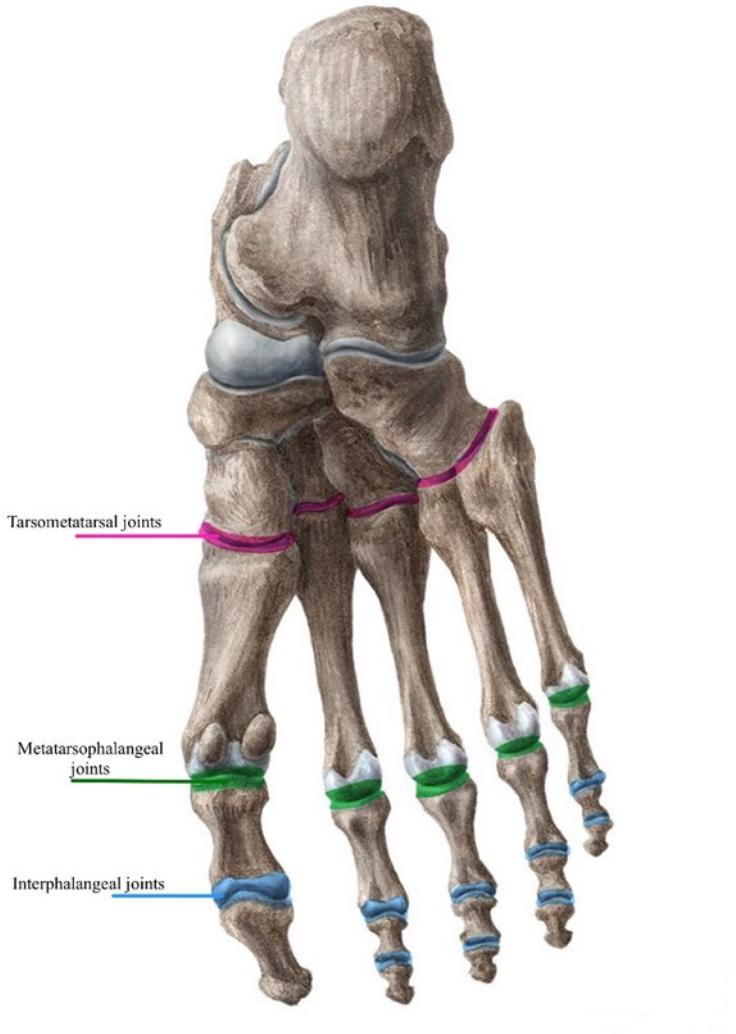

Figure 1.5: Joints of the forefoot [10].

1.1.2 Foot regions

The foot is traditionally divided into three regions: *hindfoot*, *midfoot* and *forefoot*. Moreover, the lower leg (the part between the knee and the ankle) is essential for the functioning of the foot. In figure 1.6 it is possible to see how the foot is divided.

Hindfoot

The *hindfoot* is the area between the ankle joint and the talonavicular and calcaneal-cuboid joints (together these joints are called transverse tarsal joints). The bones in this region are the talus and the calcaneus. The three parts of the talus (body, neck, and head) are designed to transmit reactive forces from the foot to the leg via the ankle joint. The calcaneus is the largest and most posterior bone of the foot, serving as a lever arm for the insertion of the Achilles tendon (this tendon is the largest and one of the strongest in the body), through which the muscles as the gastrocnemius and soleus exert

plantarflexion forces to the foot. The calcaneus's height, width, and structure allow it to sustain high tensile, bending, and compressive forces on a regular basis without any injuries.

Midfoot

The *midfoot* is the area between the transverse tarsal joint and the tarsometatarsal joint. In the midfoot there are several joints, but they all have limited mobility. The bones in this region are navicular, cuboid, and medial, middle, and lateral cuneiforms.

The midfoot stability is gained by its multi-segmental configuration, along with the connecting ligaments and muscles. [8]

Forefoot

The *forefoot* is composed of twenty-one bones: five metatarsal, fourteen phalanges, and two sesamoids. The first metatarsal is the shortest and widest. Its base, which resembles a cone, articulates with the medial cuneiform and the head articulates with the two sesamoids.

The second metatarsal grows beyond the first and articulates with the medial, lateral, and intermediate cuneiforms to increase stability, making the second ray the stiffest and most stable part of the foot.

The third, fourth and fifth metatarsals have wide bases, small shafts, and dome-shaped heads.

All toes consist of three phalanges (distal, middle, proximal), except for the hallux, which has two.

Greater stability is made possible by the heads of the proximal and middle phalanges having a trochlear shape. The toes serve as a functional component of load distribution and weight bearing. They also influence propulsion during the push-off phase of gait. [8]

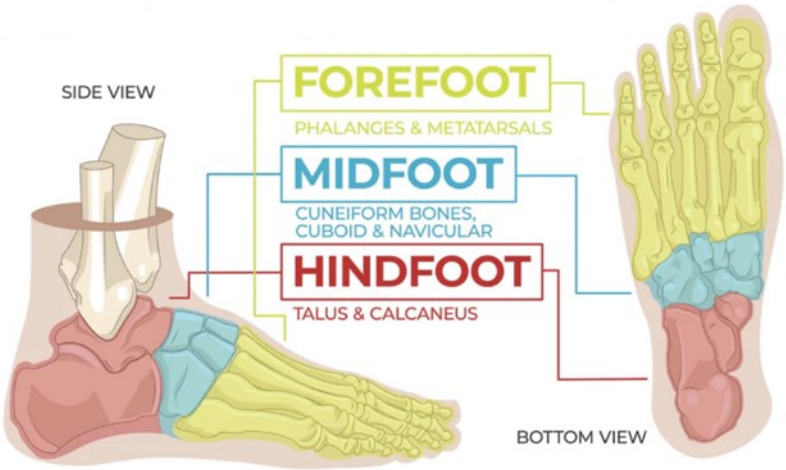

Figure 1.6: Regions of the foot [11].

1.2 Basic biomechanics of the foot

1.2.1 Basic motions

The major motion function, angulation, and support of the foot are provided by the joints of the foot, which are regulated by intrinsic and extrinsic muscles of the lower limb. As is the case with all joints, motion is produced by rotation about an axis in a plane of motion. There are three planes of motion in the foot: transverse plane, sagittal plane, and frontal plane.

The transverse plane's motions are internal rotation, or adduction of the foot, (when the distal part of the foot moves toward the midline of the leg on its vertical axes) and external rotation, or abduction of the foot, (when the end of the foot moves away from the midline of the body), these movements can be seen in figure 1.7A. The sagittal plane's motions are dorsiflexion (upward) and plantar flexion (downward) (shown in figure 1.7B), and the frontal plane's motions are inversion and eversion (shown in figure 1.7C). [12]

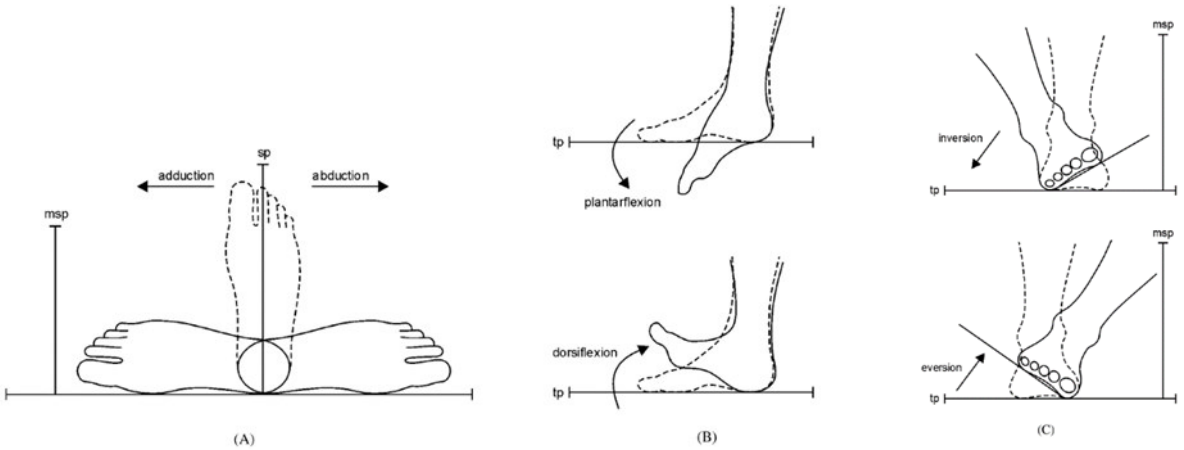

Figure 1.7: (A) Adduction-abduction, (B) plantarflexion-dorsiflexion, (C) inversion-eversion [12].

1.2.2 Joints axes

The ankle joint is the articulation between the distal section of the tibia and the body of the talus, allowing dorsiflexion and plantarflexion of the foot around its axis of motion, which runs obliquely from lateral-plantar-posterior to medial-dorsal-anterior. The minimum range of ankle joint motion required for normal locomotion is 10° of dorsiflexion and 20° of plantarflexion [12].

The subtalar axis of motion travels through the joint obliquely at roughly 42° from the transverse plane and 16° from the sagittal plane, resulting in motion in frontal plane; these motions happen simultaneously. This joint's normal motions are supination and pronation.

Ankle and subtalar axes are represented in figure 1.8.

The midtarsal joint (formed by the talonavicular and calcaneocuboid joints) has two axes of motion, one oblique and one longitudinal. These axes are not aligned with the body planes, and their relative movement results in the pronation/supination of the forefoot.

The metatarsophalangeal joints, which are formed between the rounded heads of the metatarsal bones and the shallow cavities of the phalanges, allow 90° of extension, but only a few degrees of flexion. All interphalangeal joints allow for foot extension, which is associated with abduction, and flexion, which is associated with adduction. [12]

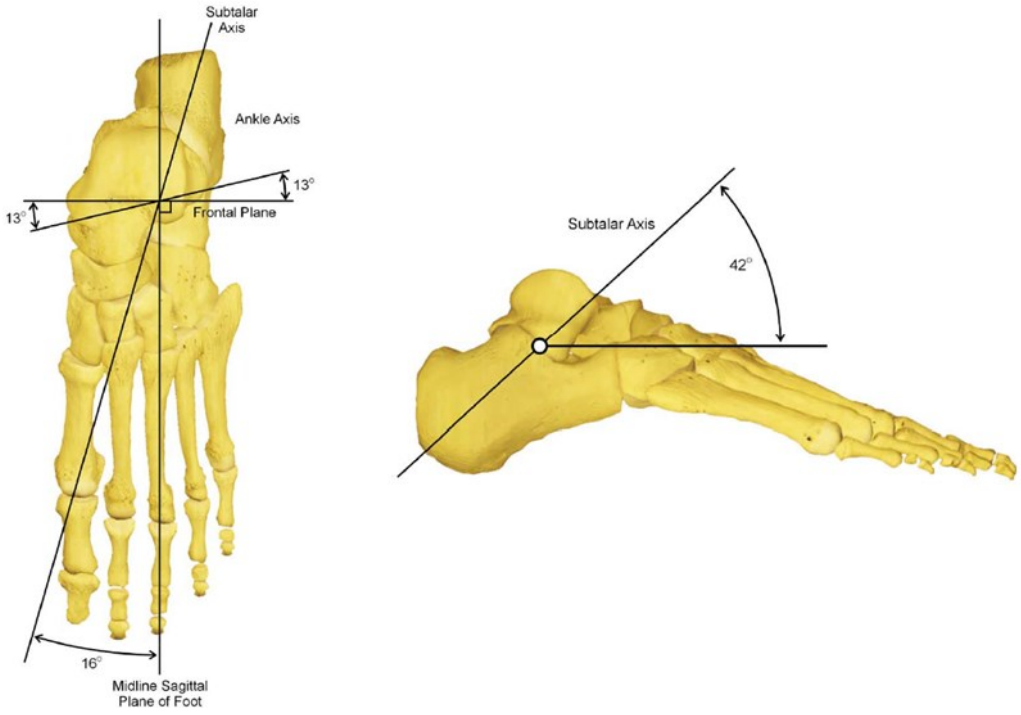

Figure 1.8: Ankle and subtalar axes [12].

Chapter 2

2. Biomechanical modelling

2.1 Overview

Computer simulation and biomechanical modelling support observations and guide experimental planning. Biomechanical models are intricate, and creating, evaluating, and researching them calls for specialist tools. [1]

Understanding the basic mechanism of movement has multiple important applications in health science and engineering: for example, to design and plan therapies for musculoskeletal disorders, to create devices that are ergonomically designed, or to improve sports training and/or equipment for athletes. While we can, relatively easily, observe human movements with so-called motion capture technologies, to measure muscle and joint reaction forces, there are not non-invasive methods [13]. Electromyography (EMG), used to measure the electric activities of muscles, has been demonstrated to show a nonlinear connection between activation and muscle force but cannot be utilized to measure muscle forces directly [14]. Recently, innovative wave speed measurement techniques have been used to non-invasively measure muscular forces for muscles close to the skin [15]. Although this technique offers some useful and direct information about the muscle force, it is only applicable to a small number of muscles and hence insufficient to fully comprehend the biomechanics of the body.

Here, musculoskeletal models allow studying the musculoskeletal system, including its tissues, structures, and interactions. With a musculoskeletal model it is possible to simulate how the body segments of a subject articulate during a dynamic task, and recover information that cannot be measured directly, such as muscle, joints, and ligaments forcers. Also, musculoskeletal models can be used to simulate disease conditions on the patients being studied, along with the resulting changes in the dynamic patterns, and compare this to simulations in healthy subjects.

Lastly, simulation technology must be adaptable and reusable for a wide range of models and movements, and these models and data should be transferable and their results reproducible.

2.2 Musculoskeletal modelling

Musculoskeletal modelling is a useful technique for studying the link between body motion and internal biomechanical loads in a variety of healthy and pathological circumstances. It has the potential to significantly improve patient care and lower treatment costs by understanding cause-and-effect links in people with neurological and musculoskeletal impairments and predicting effective surgical and rehabilitative treatments. Experiments alone cannot reveal the causes of abnormal movements, and design of treatments is limited, since crucial variables (such as muscular forces) are not frequently measured [1].

A musculoskeletal model is a mechanical description of bones, muscles, and joints that is typically used to estimate muscle and joint reaction forces (together are called internal forces) from information about the movement and external forces [13].

Different modelling software exists that can be used to create both patient-specific and generic musculoskeletal models. A patient-specific model is developed for a specific subject: the joint axes position and orientations are obtained with different methods such as computed tomography and used to build the model itself, the model is therefore based on the patient anatomy [16]. Generic models are created based on anatomical measurements of volunteers or cadavers and can be used for a wide variety of patients thanks to a process called *scaling* [17].

The program that will be used in this thesis is called OpenSim. OpenSim is one of the most used open-source software for 3D analysis of musculoskeletal systems during motion tasks.

OpenSim is a freely available musculoskeletal modeling and simulation application; Scott Delp and his collaborators (Stanford University, USA) first launched it in 2006 [1].

OpenSim is an open source and user extensible software system that allows users to develop musculoskeletal models and create dynamic simulations of movement.

The models include bones (rigids bodies), joints (mobilizers, constraint, and forces), contact elements (rigid constraints and compliant forces), as well as ligaments and muscles actuators (forces).

The software can determine variables that are hard to measure experimentally, such as muscle forces. It also allows to measure the change in length of tendons, making it possible to calculate tendon stretch and recoil during movement. OpenSim can also predict unique movements using motor control models, such as kinematic adaptations of human gait during loaded or inclined walking.

In OpenSim is possible to create musculoskeletal models, visualize their motion, and use a set of tools for obtaining useful data. The *Inverse kinematics* tool is used to calculate internal coordinates from available spatial marker positions (e.g., skin markers data), corresponding to known landmarks on rigid segments; *inverse dynamic* allows calculating a set of generalized forces required to match the

estimated accelerations; *static optimization* decomposes the net generalized forces among redundant actuators (muscles); and *forward dynamics* constructs state trajectories in response to input controls and external influences by integrating system dynamical equations. Specialized tools are available to create patient-specific simulations. Scaling an existing model to fit patient-specific measurements or determining dynamic muscle activations that lead the model to track experimental data are two examples [1]. All these tools will be explained in more detail later in this thesis.

A model created in OpenSim, even if personalized, is an approximation of the human musculoskeletal system, and its validity is dependent on the following assumptions:

- Body segments are considered as rigids bodies: this means that they are not deformable under internal or external loading (bone deformations are assumed to have little impact on joint articulations or muscle force estimations).
- By assuming that the bones are rigid, Newton's law of motion can be used to describe the connection between the forces and moments acting on the segments and their linear and angular accelerations [13].
- The length of the body segments is measured as the distance between anatomical landmarks.
- The mass of the body segments is designed to be always concentrated in the middle of the segment itself, during dynamics. This is not what happens in real conditions, where the centre of mass is not constant but changes its position over time.
- The motion of soft tissues, such as skin, fat, and muscles, is ignored.
- The sliding between bones is ignored, there is no friction in the joints [18].
- Muscles are modelled by the Hill phenomenological model, which describe both the elastic properties of the tissues as well as the contractile element [13].

In the figure 2.1 the key elements of a typical musculoskeletal simulation in OpenSim are shown. It is known that human movement is the result of a complex orchestration of the neural, muscular, skeletal, and sensory system; OpenSim includes computational models of these systems, allowing for the analysis and prediction of movement.
With experimental data, such as electromyogram, or controller models it is possible to estimate the neural commands to muscles (in the form of excitations). In OpenSim the musculotendon models follow Hill-type models, which translate excitation into muscle forces. Lastly, there are several solvers/integrators that allow users to generate muscle-driven simulations (forward simulation) or solve for muscle forces and moments that produce observable motion (inverse simulation) [6].

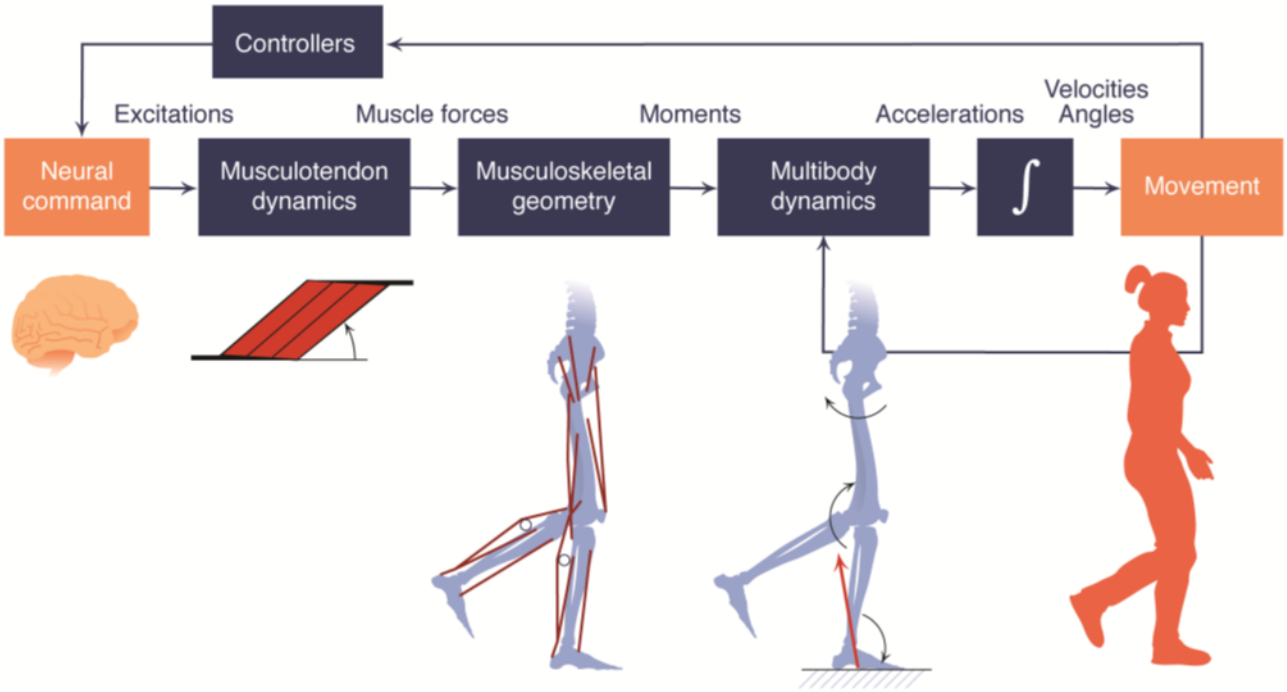

Figure 2.1: Elements of a typical musculoskeletal simulation in OpenSim [6].

Some models can be freely available, if the developers share them, and are frequently utilized for multiple investigations since they provide a rich set of movements that allow for multiple paths of research. OpenSim provides a wide variety of models, depending on the type of analysis required: it is possible to choose models that depict upper limbs or lower limbs of the body. Therefore, it is important to choose the model that best suits the research question.

OpenSim allows for a wide variety of simulations, such as scaling, inverse kinematics, inverse dynamic, and forward dynamic. The first three analyses will not be used in this work, but it is still important to briefly explain what they are.

2.2.1 Scaling

When working with a generic model it is possible to scale the model using subject specific data, in order to conduct a meaningful motion simulation.

The scaling tool in OpenSim is a multi-stage process to scale multiple characteristics of the model to fit the patient data as closely as possible. Typically, scaling is implemented by comparing experimental marker data (obtained using motion capture equipment) to virtual markers placed in the same anatomical location in the unscaled model; this way the model's dimensions are scaled so that the distances between virtual markers match the distances between experimental markers. The mass of each segment is scaled as well.

The steps required to scale the model are:

1. Compute the scale factors for each body segment. It can be achieved by combining measurement-based (scale factors are determined by comparing distances between markers on the model and experimental marker positions) and/or manual scaling.
2. Scaling the model's geometry based on computer scale factors.
3. Scaling mass and inertial properties.
4. Scaling muscles and other model components that depend on length (like ligaments and muscle actuators) [19].

In the figure below is possible to see a schematic illustration of the inputs required for the scaling tool to function s well as the file generated by the scaling tool itself:

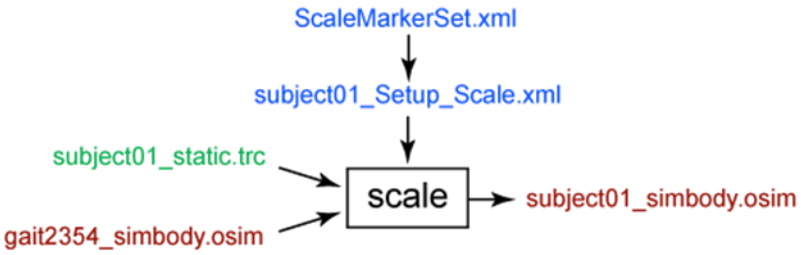

Figure 2.2: Scaling tool. The experimental data is shown in green; OpenSim files are in red; settings files are in blue.
'gait2354_simbody.osim' is the generic model in input, 'subject01_simbody.osim' is the model that has been scaled to match the experimental data that are contained in 'subject01_static.trc' [19].

2.2.2 Inverse kinematic

Kinematics is the study of motion without taking into consideration the forces and moments that cause it. Therefore, mass and inertia properties are not required to conduct kinematical analysis such as inverse kinematics. The goal of inverse kinematics is to determine the model's joint angles that best reproduce the experimental kinematics of a specific subject.

The Inverse Kinematics (IK) tool iteratively goes through each time frame of experimental data, positioning the set of joint angles that put the model in a configuration that "best matches" the experimental marker and coordinates data for that time step. This "best match" pose is the one with the lowest sum of weighted squared errors, whose solution seeks to reduce both marker and coordinate errors: the goal is to minimize the *marker error*.

Marker error is defined as the distance between an experimental marker and the equivalent virtual marker. Each marker has a weighting value that specifies how strongly the error term of that marker should be minimized in the least squares problem [20].

The weighted least squares problem solved by IK is:

$$min\left[\sum_{i=1}^{\#markers} w_i\left\|x_i^{exp} - x_i(q)\right\|^2 + \sum_{j=1}^{\#coordinates} \omega_j\left(q_j^{exp} - q_i\right)^2\right] \text{[21]}$$

Where:

- q is the vector of generalized coordinates (e.g., joint angles).
- x_i^{exp} is the position of *experimental marker i*.
- $x_i(q)$ is the position of the corresponding *virtual marker i*.
- q_j^{exp} is the *experimental value* for coordinate *j*.
- w_i and ω_j are the weight of marker and coordinate respectively [21].

In the figure below is possible to see a schematic illustration of the inputs required and outputs for the IK tool to function:

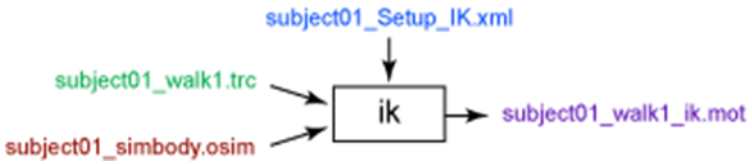

Figure 2.3: Inputs and outputs of the IK tool. The experimental data is shown in green; OpenSim files are in red; settings files are in blue; files generated by the workflow are shown in purple [21].

The inputs of the tool are:

- *'subject01_simbody.osim'* is a subject specific scaled generic model.
- *'subject_walk1.trc'* are experimental marker trajectories for a trial generated from a motion capture system, associated with the time range of interest.
- *'subject01_Setup_IK.xml'* is a file containing the settings information for the IK tool, including the marker weightings.

The output is:

- *'subject01_walk1_ik.mot'* is a motion file containing the generalized coordinate trajectories generated by IK (joint angles and translations).

2.2.3 Inverse Dynamics

Dynamic is the study of motion as well as the forces and moments that cause it. Therefore, estimation of mass and inertia is essential to perform dynamic analysis such as inverse dynamics.

Inverse dynamics is used to estimate the forces and moments that create a specific motion, and the results can be used to infer how muscles are used for that motion. To determine these forces and moments, equations of motion for the system are solved iteratively.
The Inverse Dynamic (ID) tool calculates the generalized forces at each joint that cause a particular movement, by solving the equations of motion (F=ma) [20].

In the figure below is possible to see a schematic illustration of the inputs required and outputs for the ID tool to function:

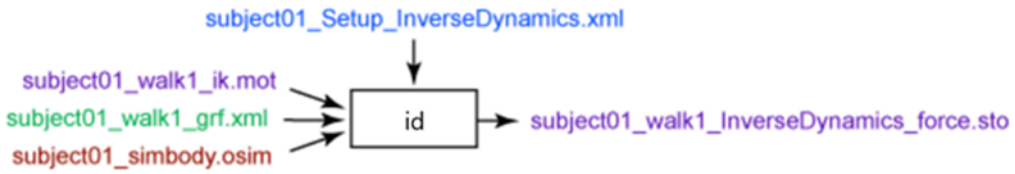

Figure 2.3: Input and outputs of the inverse dynamics tool. The experimental data is shown in green; OpenSim files are in red; settings files are in blue; files generated by the workflow are shown in purple [22].

The inputs of the tool are:

- *'subject01_walk1_ik.mot'* is a motion file that contains the time histories of generalized coordinates that describe the model's movement.
- *'subject01_walk1_grf.xml'* is a file containing the external loads data (i.e., ground reaction forces, moments, and centre of pressure location)
- *'subject01_simbody.osim'* is a subject specific scaled generic model.

The outputs are:

- *'subject01_walk1_InverseDynamics_force.sto'* is a storage file containing the time histories of the net joint torques and forces acting along the coordinate axes to produce the estimated accelerations.

2.2.4 Residual Reduction

Residual reduction is a type of forward dynamic simulation that uses a tracking controller to follow model kinematics determined by inverse kinematics.
The goal of residual reduction is to reduce the effects of modelling and marker data processing errors, which accumulate and result in significant nonphysical compensatory forces, known as *residuals*. Residual reduction modifies the torso mass centre of a subject-specific model and allows the model's kinematics from Inverse Kinematics to vary in order to be more dynamically consistent with the ground reaction force data.

Residual reduction is intended primarily for gait, where the model is moved relative to the ground while subject to ground reaction forces and torques. For example, is it possible to take a gait model (i.e., gait2354_simbody.osim) that is composed of ten rigid segments, and has 23 degrees of freedom (DOF). 17 of these DOF are actuated each by a one torque actuator; the remaining 6 represent the DOF between pelvis and the ground (3 translational, 3 rotational). Is it possible to represent these as a 6-degree-of-freedom joint and actuate each DOF with its own torque actuator. Each of these actuators is called *residual actuator*.

The residuals that actuate the 3 transitional degrees of freedom between the pelvis and the ground are called *residual forces*, and their values are indicated by Fx, Fy, and Fz (which are the forces along x,y, and z axis respectively). The 3 rotational degrees of freedom are actuated by the residual torques (or moments), whose values are indicated by Mx, My, and Mz.

RESIDUAL REDUCTION ALGORITHM (RRA)

1. Tracking simulation

   RRA starts by setting the model's generalized coordinates to the values calculated by the inverse kinematics tool for the user-specific initial time. RRA iteratively advances in time (with each time step of .001) until the user-specified final time is reached.

   Each step computes force values for all the model's actuators in order to move the model from its current configuration to the desired configuration (generalized coordinates) at the conclusion of the step, which is computed from the IK output. The actuator forces are calculated by selecting force and torque values that minimise a function.

2. Mass centre adjustment

   The average value for each residual actuator is calculated at the end of the simulation.

   The average values for Mx (left-right residual torque) and Mz (fore-aft residual torque) are used to adjust the torso mass centre to rectify excessive "leaning" of the model due to flaws in the model's mass distribution and torso geometry. A new model file is created with the altered torso mass centre.

3. Mass adjustment recommendation

   The suggested mass changes for all body segments are calculated using the average value of Fy. The desired mass change is $^{Fy}/_{g}$ where g=-9.80665 m/s^2. This mass change is then proportionally distributed throughout the body segments.

4. Adjusted kinematics

   The tracking simulation method is then repeated, but with three key differences:

   - The model with the adjusted torso mass centre is used.

- The weight on the residual is heavier to force the optimizer to choose smaller values of residuals when minimizing the objective function.
- The residual values are subjected to minimum and maximum constraints.

The purpose of these residual value constraints is to decrease the need for residuals to the absolute minimum that is required to closely follow the specified kinematics, so that motion is created solely by internal joint moments [23].

The figure below depicts the inputs and outputs required to run the residual reduction algorithm:

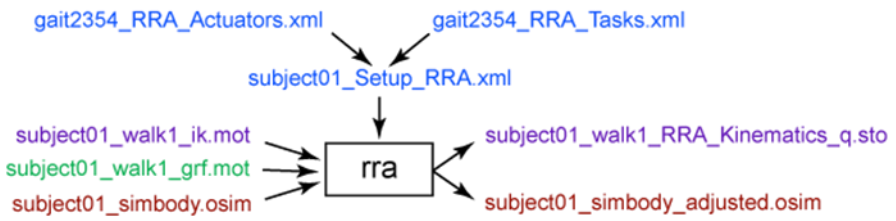

Figure 2.4: inputs and outputs for performing RRA. The experimental data is shown in green; OpenSim files are in red; settings files are in blue; files generated by the workflow are shown in purple [24].

The setting files are:

- *'subject01_setup_RRA.xml'* is a setup file for the RRA tool, that contains specific settings, inputs, and outputs that affect the behaviour of the RRA.

  The actuators and kinematic tracking are identified in the setup files. Control constraints on the actuators can also be provided (to limit the maximum residual force).

The inputs of the tool are:

- *'subject01_walk_ik.mot'* is a file that contains the time histories of the model kinematics (i.e., joint angles and pelvis translations).
- *'gait2354_RRA_Tasks.xml'* is a tracking task file that specifies which coordinates to track and the tracking weight (weights are relative, and they affect how "well" a joint angle tracks the specified joint angle from IK). In this file it is also possible to specify further constraints on the RRA actuators. On this topic, is important to make some considerations:
  i. Selection of the values kp and kv are not arbitrary: they define the behaviour of the error dynamics and can be written in terms of system poles. For a stable critically damped system (real negative poles), kp = λ^2 and kv = -2λ.
  ii. Kinematics of joints for which we have more confidence (knee flexion, hip flexion) are weighted more heavily than those in which we have less confidence (hip internal rotation, ankle inversion).
  iii. Joint torques (and muscles) have a maximum magnitude of 1.

- *'subject01_walk1_grf.xml'* is a file that specifies the measured ground reaction forces that should be applied to the model during simulation, as well as how they should be applied.
- *'subject01_simbody.osim'* a scaled subject specific OpenSim model.
- *'gait2354_RRA_actuators.xml'* are ideal joint actuators used to replace muscles. The Actuator Set defines the residual and reserve actuators that will be used, as well as their properties such as maximum/minimum force and body, joint, or location.

The outputs are:

- *'subject01_adjusted.osim'* a model with adjusted mass properties (is an optional output).
- A series of files that contain data about: adjusted kinematics and corresponding model states of the simulated motion (i.e., joint angles, velocities, and accelerations); actuator excitations, forces and torques; summary of the average residual values; position errors for each of the model's generalized coordinates during the trial [24].

2.2.5 Forward Dynamics

In forward dynamics, a mathematical model describes how coordinates and their velocities change according to applied forces and torques, as opposed to inverse dynamics, where the motion of the model was known and we wanted to discover the forces and torques that created the motion (moments).

From Newton's second law, is it possible to describe the accelerations of the coordinates in terms of the inertia and forces that act on the skeleton as a set of rigid bodies (multibody dynamics):

$$\ddot{q} = [M(q)]^{-1}\{\tau + C(q,\dot{q}) + G(q) + F\}\ [25]$$

Where:

- q is a function of coordinates.
- $\ddot{q}$ is a function of the coordinate accelerations due to joint torques τ.
- $C(q,\dot{q})$ Coriolis and centrifugal forces.
- $G(q)$ gravity.
- F other forces applied to the model.
- $[M(q)]^{-1}$ the inverse of the mass matrix.

The Forward Dynamics (FS) Tool can drive a forward dynamic simulation in response to the controls (such as muscle excitations) generated by the Computed Muscle Control or another method.

The goal of Computed Muscle Control (CMC) is to calculate a series of muscle excitations (or, more generally, actuator commands) that will drive a dynamic musculoskeletal model to follow a specified set of kinematics while external forces are being applied.

A forward dynamics simulation is the solution of the differential equations that define the dynamics of a musculoskeletal model. By doing this, more in-depth biomechanical data for the experiment in question can be gathered by focusing on particular time windows of interest and by applying different analyses.

The basic analyses of interest are:

- **Kinematics**: register the generalized coordinates (q), generalized speeds (u) and accelerations ($^{du}/_{dt}$).
- **BodyKinematics:** keeps track of each body's configuration, including its centre of mass position and orientation, as well as its linear and angular velocities and accelerations (linear and angular). It also keeps track of the model's total centre of mass, along with its acceleration and velocity.
- **Actuation:** register the generalised force, speed, and power generated by each model actuator. The generalized force can either be a force (measured in N) or a torque (measured in Nm). The actuator's speed is the rate at which the actuator shortens and can be translational (m/s) or angular (rad/s). The rate at which an actuator executes work is measured in Watts. Positive work indicates that the actuator is supplying energy to the model, while negative power indicates that the actuator is taking energy from the model [26].

The figure below depicts the inputs and outputs required to run the forward dynamics tool:

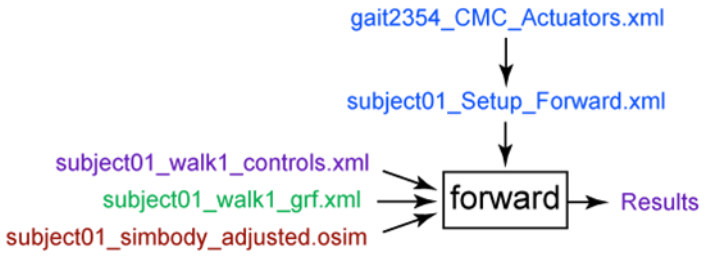

Figure 2.5: inputs and outputs for performing forward dynamic. The experimental data is shown in green; OpenSim files are in red; settings files are in blue; files generated by the workflow are shown in purple [25].

The inputs of the tool are:

- *'subject01_walk1_controls.xml'* is a file that contains the time histories of the model controls (e.g., muscle excitations) to the muscles and/or joint torques. This file may be generated by the user, the Static Optimization tool, or the Computer Muscle Control tool.
- *'subject01_walk1_states.sto'* is a file that contains the time histories of the model states, including joint angles, joint speeds, muscle activation, and muscle fibre lengths. These states are used by the FS tool to establish the initial states of the model. If no initial states file is specified, the simulation will start from the default pose of the model.

- *'subject01_walk1_grf.xml'* is a file that describes the external loads that are applied (like measured ground reaction forces).
- *'subject01_simbody_adjusted.osim'* a scaled subject specific OpenSim model.
- *'subject01_Setup_Forward.xml'* is a setup file for FS tool [25].

2.3 Foot and ankle musculoskeletal models

In this work the attention is focused on the foot musculoskeletal model, thus it is important to understand the different types of models that are currently available and choose what fits best.

2.3.1 Traditional musculoskeletal foot model

The traditional foot musculoskeletal model is part of the Gait 2392 model, which represents the lower extremities and torso. It was created by Darryl Thelen et al. (Stanford University) [27].

The Gait 2392 model has 23 degrees of freedom and has seven rigid-body segments: pelvis, femur, patella, tibia\fibula, talus, foot (which includes calcaneus, navicular, cuboid, cuneiforms, metatarsals), and toes.

The foot however is only described by three segments. Also, out of all the joints that the anatomical foot, in this model only three are defined: the ankle, subtalar and metatarsophalangeal joints. These joints are modelled as frictionless revolute joints with axes oriented as shown in the figure below. They have 1 degree of freedom each, for a total of 3 degrees of freedom for the whole foot. The 3 DOF are plantarflexion\dorsiflexion in the ankle and in the metatarsophalangeal joint and inversion\eversion in the subtalar joint. [27].

In this model are also included the extrinsic foot muscles: medial gastrocnemius, lateral gastrocnemius, soleus, tibialis posterior, tibialis anterior, peroneus brevis, peroneus longus, extensor digitorum, and extensor hallucis [28].

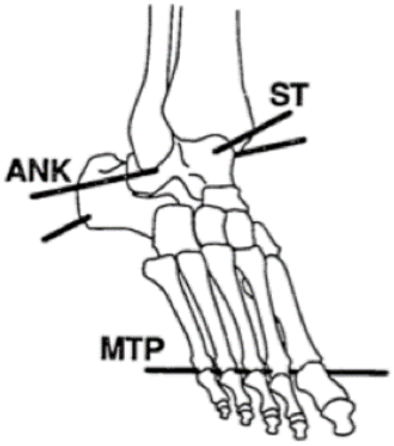

Figure 2.2: Ankle, subtalar, and metatarsophalangeal joints axes [27].

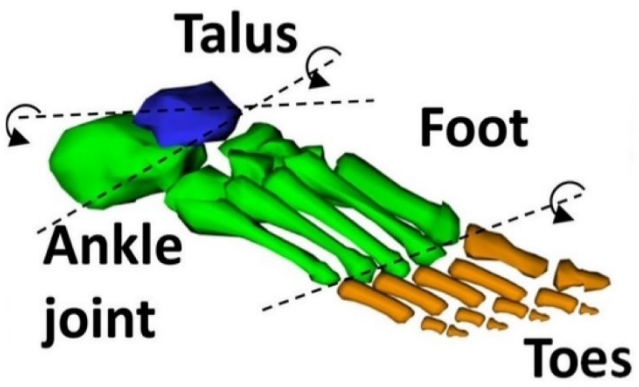

Figure 2.3: Traditional foot model [27].

2.3.2 Extended multibody musculoskeletal foot model

The foot is a highly complex structure, and the traditional musculoskeletal model oversimplifies the foot kinematics and dynamics. Due to the complexity of the construction, a small number of bodies is often insufficient to capture the intricacy of human foot motion and joint loading.

For this reason, an extended model was introduced. This model was developed by Tiago M. Malaquias et al. [3] and was generated based on CT scans from one healthy subject, then validated by motion capture data collected in five healthy subjects.

In Malaquias's study two models were compared, both with the same structure, but with 15 and 8 degrees of freedom (DOF). Since the model with 8 DOF resulted in kinematics that better resembled literature, only this will be described.

This model consists of six rigid bodies: shank (tibia and fibula), talus, calcaneus, midfoot (cuboid, navicular, and cuneiforms), forefoot (metatarsal) and toes. It has five anatomical joints: ankle, subtalar, midtarsal, tarsometatarsal, and metatarsophalangeal.

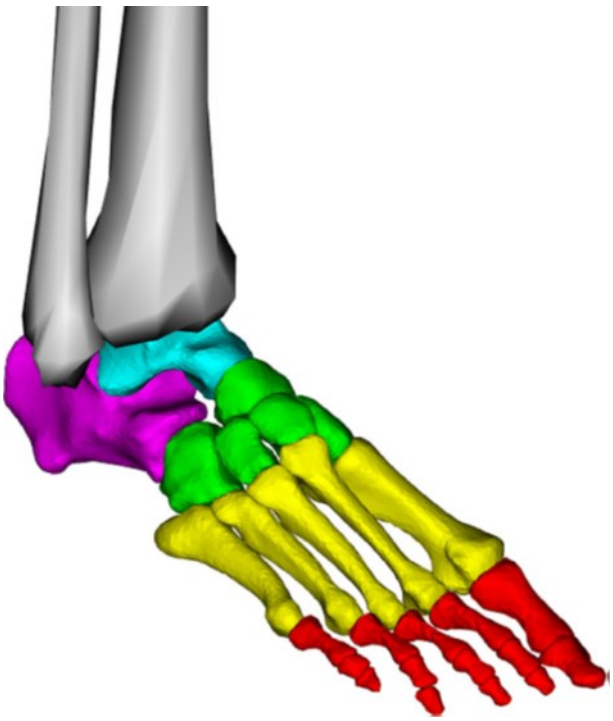

Figure 2.4: Extended foot model. The segments of the model are: light blue - talus; purple - calcaneus; green - midfoot; yellow - forefoot; red – toes [3].

The 8 DOF of the model are distributed on the model joints following the work of Hicks [29].
The DOF are distributed:

- One DOF at the ankle joint, that allows plantarflexion and dorsiflexion.
- One DOF at the subtalar joint, that was defined by an oblique axis. Resulting in a combination of eversion-abduction-extension and inversion-adduction-flexion.
- Two DOF at the midtarsal joint, defined by two axes (one oblique and one anterior-posterior). These axes allow a combination of eversion-abduction- extension and inversion-adduction-flexion.
- Two DOF at the tarsometatarsal joint, defined by two axes (the 1st ray axis and the 5th ray axis). These axes allow both flexion-eversion and extension-inversion.
- Two DOF at the metatarsophalangeal joint, that allow plantarflexion\dorsiflexion and abduction\adduction.

There are also thirty-six ligaments defined in the models; their geometrical path and resting length are described in the table 2.1. The resting length is presented for the generic model before scaling [3].

Ligament	Origin	Via points	Insertion	Resting length (m)
Tibio-talar posterior	Tibia	–	Talus	0.01982
Tibio-talar anterior	Tibia	–	Talus	0.02534
Tibio-calcaneal	Tibia	–	Calcaneus	0.03015
Tibio-navicular	Tibia	–	Navicular	0.04080
Talo-fibular posterior	Tibia	–	Talus	0.03009
Talo-fibular anterior	Tibia	–	Talus	0.03016
Calcaneo-fibular	Tibia	–	Calcaneus	0.03571
Plantar fascia	Calcaneus	First metatarsal	First prox. phalange	0.14290
Plantar fascia	Calcaneus	Second metatarsal	Second prox. phalange	0.14404
Plantar fascia	Calcaneus	Third metatarsal	Third prox. phalange	0.14335
Plantar fascia	Calcaneus	Fourth metatarsal	Fourth prox. phalange	0.13612
Plantar fascia	Calcaneus	Fifth metatarsal	Fifth prox. phalange	0.12815
Longitudinal plantar	Calcaneus	Cuboid	Second Metatarsal	0.08037
Longitudinal plantar	Calcaneus	Cuboid	Third metatarsal	0.07665
Longitudinal plantar	Calcaneus	Cuboid	Fourth metatarsal	0.07153
Longitudinal plantar	Calcaneus	Cuboid	Fifth metatarsal	0.06389
Calcaneo-navicular plantar	Calcaneus	–	Navicular	0.01968
Calcaneo-navicular plantar	Calcaneus	–	Navicular	0.01214
Calcaneo-navicular plantar	Calcaneus	–	Navicular	0.01041
Calcaneo-cuboid plantar	Calcaneus	–	Cuboid	0.01767
Calcaneo-cuboid plantar	Calcaneus	–	Cuboid	0.02296
Calcaneo-cuboid dorsal	Calcaneus	–	Cuboid	0.02543
Talo-navicular dorsal	Talus	–	Navicular	0.01164
Talo-navicular dorsal	Talus	–	Navicular	0.01164
Calcaneo-navicular bifurcate	Calcaneus	–	Navicular	0.01659
Calcaneo-cuboid bifurcate	Calcaneus	–	Cuboid	0.01422
Tarsometatarsal dorsal	Medial cuneiform	–	First metatarsal	0.01271
Tarsometatarsal dorsal	Inter. cuneiform	–	Second metatarsal	0.00963
Tarsometatarsal dorsal	Lateral cuneiform	–	Third metatarsal	0.00684
Tarsometatarsal dorsal	Cuboid	–	Fourth metatarsal	0.00852
Tarsometatarsal dorsal	Cuboid	–	Fifth metatarsal	0.00733
Tarsometatarsal plantar	Medial cuneiform	–	First metatarsal	0.00903
Tarsometatarsal plantar	Inter. cuneiform	–	Second metatarsal	0.00745
Tarsometatarsal plantar	Lateral cuneiform	–	Third metatarsal	0.00697
Tarsometatarsal plantar	Cuboid	–	Fourth metatarsal	0.00767
Tarsometatarsal plantar	Cuboid	–	Fifth metatarsal	0.00897

Table 2.1: Ligaments geometrical path description [3].

After seeing both models, it is clear that the extended multibody foot model gives a better description of the complex structure that is the anatomical foot. Therefore, Malaquias's model will be the base for the project discussed in this thesis.

2.4 Validation of musculoskeletal models

Musculoskeletal models are used to simulate movement and to collect data or information that is difficult to gather experimentally; the output of a model can be used to determine the approach for a surgical procedure or have a direct influence on diagnostics and treatment decisions. Therefore, they are becoming increasingly important in orthopaedics decision-making processes. This achievement necessitates to assume that the models are accurate representations of the of the systems they simulate. In fact, if the model generates erroneous predictions, these can have serious consequences for diagnostical and surgical planning. A computational model will achieve its full potential only when it is deemed dependable enough to not necessitate experimental validation of each new result.
This can be obtained with a verification and validation process, that it is the method used to determine the accuracy and reliability of musculoskeletal models:

- Model verification is focused on how the model is implemented as well as the numerical accuracy of the answer.
- Model validation is the process of establishing how well a model accurately represents real-world and experimental data [5].

In this thesis the main focus was validating a foot musculoskeletal model using data acquired by Boey et al. [2] with 4D CT combined with an actuated foot manipulator. Therefore, the focus of this paragraph will be only the validation process of a model.
The primary purpose of a validation process is to evaluate the computer simulation's capacity to predict specific variables of interest. So, the comparison of computational outputs with experimental data to quantify variability and errors in the computational model is the major issue of validation. Another feasible experimental approach for validating these models is to systematically adjust one or more parameters and monitor an output measure as a function of those parameters [30].
The validation process can be divided into three main stages:

- Comparison between computational and experimental outputs.
- Extending the model prediction to the conditions under which the model is meant to be employed.
- Deciding whether the precision is adequate for the intended application.

There are two types of validation: direct and indirect validation. Direct validation occurs when a model output of interest can be directly compared to an experimental measurement of the same quantity, e.g., joint reaction forces. An example of indirect validation is the comparison of EMG measurements with predicted muscle forces to infer confidence in joint compressive force calculation. Since the same model can be used for different applications, it is important to highlight that the validation should also be a responsibility of the final user of the model. There is no definitive way of determining what level of accuracy is required for a model to be considered validated: The precision required is determined by the application, not by the model itself [5].

Chapter 3

3. Application of biomechanical modelling to the foot-ankle complex

3.1 Introduction

Biomedical modelling is mostly used to study motion analysis. Motion analysis is a science that characterises, analyses, and defines human movement: it can be used to evaluate different motion patterns such as walking (gait analysis), athlete performance, and different types of human movement. After observing the motion, it is possible to use musculoskeletal models to deepen the data that we can obtain with motion analysis (i.e., joint angles).

Motion analysis also seeks to determine the angles of the joints by observing articular movements. After this research, using additional tools like musculoskeletal modelling, would it be feasible to determine the forces generated by the individual muscles that control the task under study and the weights pressing against the soft tissues.

An example of the use of motion analysis is individual foot bone kinematics analysis; this analysis is useful for detecting joint instabilities, assisting in pre-operative and post-operative evaluation of these instabilities, and studying the influence of joint degeneration or treatment approaches on hind and midfoot function.
Unfortunately, the small size of many of the foot-bones, as well as the complexity of their articular processes, complicates measurements of foot motion. Difficulties in reliably quantifying foot motion have limited progress in the diagnosis and treatment of common foot diseases.

To evaluate foot kinematics, it is possible to use different methods, two of them are:

- 3D motion capture using detailed skin markers.
- Medical imaging, such as static computer tomography (CT) or dynamic computer tomography (4DCT).

3.2 Gait Analysis

Gait analysis is the study of human locomotion. Walking is a complicated combination of muscle forces on bones, rotations through several joints, and physical forces acting on the body. Gait analysis, which can be accomplished through simple observation or three-dimensional analysis with measurements of joint angles (kinematics), joint forces (kinetics), muscular activity, foot pressure, and energetics (measurement of energy used during an activity), enables the physician to create procedures that are specific to the demands of each patient.

Gait analysis provides objective data for preoperative and postoperative outcome assessment. This data can also be used to develop orthotic and new surgical techniques.

When studying foot motion, gait analysis is really important to evaluate possible joint instabilities and harmful patterns of gait that can lead to joint degradation.

3.2.1 Gait cycle

To evaluate and quantify how someone walks, the shortest, unique, and repeatable task during gait must be isolated: this is known as the gait cycle. Conventionally, gait cycle is measured from one foot strike to the subsequent foot strike of the same foot.

Understanding the gait cycle and its many phases is necessary to ensure an effective gait analysis.

The gait cycle can be divided into two different primary phases: the stance phase and the swing phase, which alternate for each lower limb.

- Stance phase: this term is used to designate the entire period during which the foot is on the ground. It begins when the foot first hits the ground and finishes when the same foot leaves the ground. The stance phase accounts for roughly 60% of the gait cycle.
- Swing phase: this term is used for the time the foot is in the air for limb advancement. It begins when the foot first leaves the ground and finishes when the same foot strikes the ground again. The swing phase accounts for the remaining 40% of the gait cycle.

Observing both the spatial and temporal properties of the two lower limbs allows for the introduction of complementing phases.

The right foot makes initial contact while the left foot remains on the ground, and there is a time of *double support* (also known as *double limb stance*) between the right's initial touch and the left's toe off. During the swing phase on the left side, only the right foot is on the ground, resulting in a time of *right single support* (or *single limb stance*), which terminates with initial contact by the left foot.

Then there's another time of double support, until the right foot's toe-off. The cycle ends with the following initial touch on the right, which corresponds to the right swing phase and *left single support* phase [31].

In the table 3.1 is possible to see the percentages that characterize the phases of the gait circle. Is important to mention that these percentages may vary as the walking speed increases: the swing phase becoming proportionally longer, while stance phase and double support phases becoming shorter. The disappearance of the double support phases represents the transition from walking to running.

Gait cycle phases		
Stance		60%
Initial double support	10%	
Single support	40%	
Terminal double support	10%	
Swing		*40%*

Table 3.1: Phases of the gait cycle **[32]**.

The two main phases (stance and swing) are usually divided into eight more phases, five referring to the stance phase and three to the swing phase.
The stance phase includes:

- Initial contact
- Loading response
- Midstance
- Terminal stance
- Pre swing

The swing phase includes:

- Initial swing
- Mid swing
- Terminal swing

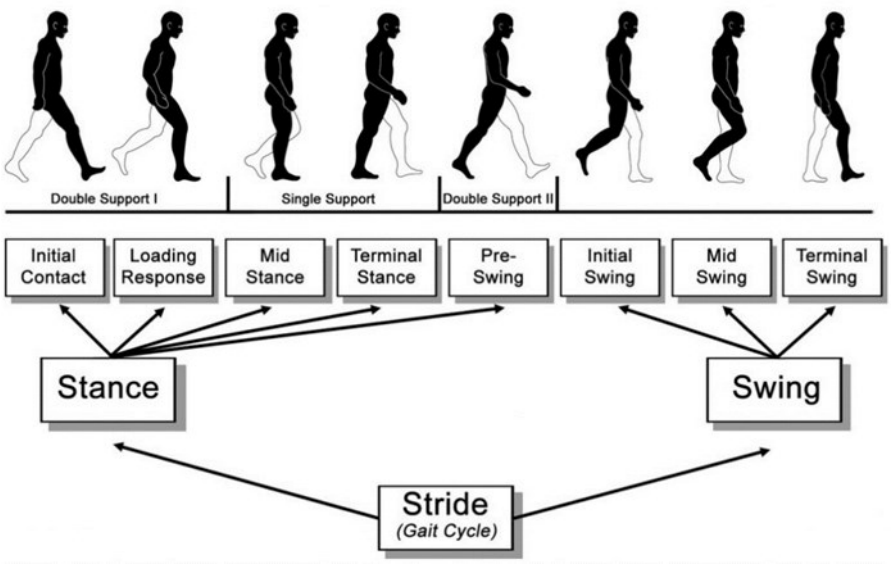

Figure 3.1: schematic representation of the gait cycle [33].

PHASES OF THE GAIT CYCLE

Each of the eight gait phases has a functional aim and a key pattern of selective synergistic motion to achieve it. The sequential arrangement of the phases also allows the limb to perform three basic tasks: weight acceptance, single limb support, and limb advancement.

Weight acceptance (0-12%)

The goals of weight acceptance are to stabilize the limb, shock absorption, and maintain the progression of the body. The challenge arises from the sudden transfer of body weight onto a limb that has just finished swinging forward and has an unstable posture. This phase is further subdivided into initial contact and loading response.

- **Initial contact**

  The initial contact (also known as heel-strike) is a brief period of the stance that occurs when the foot hits the ground and is the first phase of double support (the contralateral foot is still touching the ground). This phase consists of the first 3% of the gait cycle.

  The hip is flexed, the knee is extended, and the ankle goes from dorsiflexed to neutral during this phase. This phase includes the instant when the foot just makes contact with the floor, the first part of the foot to touch the ground is the heel. The joint postures present at this moment determine the loading response pattern of the limb.

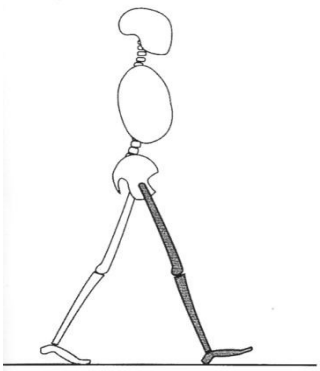

Figure 3.2: Initial contact. Shading indicates the reference limb. The other limb (clear) is at the end of terminal stance [31].

- **Loading response**

  The loading response (also known as foot flat) is the phase of the gait cycle where the body weight is transferred onto the forward limb; it goes from 3-12% of the cycle.

  In this phase, the knee flexes to adsorb shock as the foot falls flat on the ground, stabilizing in advance for single limb support. The ankle plantar flexion limits the heel rocker by forefoot contact with the floor. This phase ends the initial double stance period.

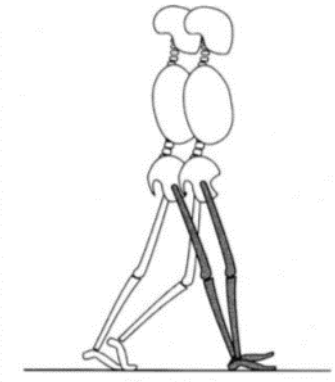

Figure 3.3: Loading response. shading indicates the reference limb. the other limb is in pre-swing phase [31].

Single limb support (12-50%)

Single limb support involves progression of the body over the foot and maintaining weight-bearing stability. The single limb support interval for the stance limb begins when the opposite foot is lifted for swing. This continues until the opposite foot makes contact with the floor again.

Two phases are involved in the single limb support: midstance and terminal stance.

- **Midstance**

  Midstance is the first half of single limb support, and it goes from 12-31% of the gait cycle.

While the knee and hip extend, the limb advances over the fixed foot by ankle dorsiflexion (ankle rocker). The opposite limb is in the middle of its swing.

It starts with lifting the opposite foot and continues until the body weight is aligned over the forefoot.

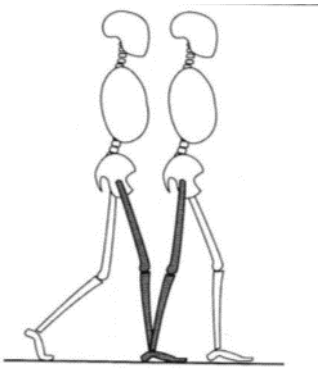

Figure 3.4: Midstance [31].

- **Terminal stance**

  Terminal stance (also called heel-off phase) is the second stage of single limb support and goes from 31-50% of the gait cycle.

  The centre of mass advances out in front of the supporting foot during terminal stance. The heel rises as the limb progresses across the forefoot rocker and the knee extends further and then begins to flex slightly. Increased hip extension causes the limb to trail more. The opposite limb is in full swing.

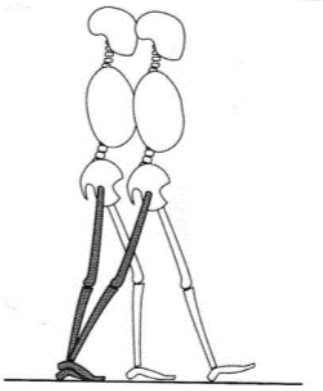

Figure 3.5: Terminal stance [31].

Limb advancement (50-100%)

Preparatory posturing begins in stance to meet the high demands of advancing the limb. The limb then swings through three postures as it rises itself, moves forward, and prepares for the following stance phase. Four phases are involved: pre swing, initial swing, mid swing, and terminal swing.

- **Pre swing**

The pre swing phase (also known as toe-off phase) takes place during 50-62% of the gait cycle. This final phase of stance is the second (and terminal) double stance of the gait cycle. It starts with initial contact of the opposite limb and terminates when the toes of the reference limb leave the ground. The phase's goal is to prepare the leg for the swing phase: in the reference limb there is an increase in ankle plantar dorsiflexion, greater knee flexion and loss of hip extension.

The body weight is transferred abruptly to the opposite leg and the unloaded limb takes advantage of its mobility to prepare for the rapid demand of swing.

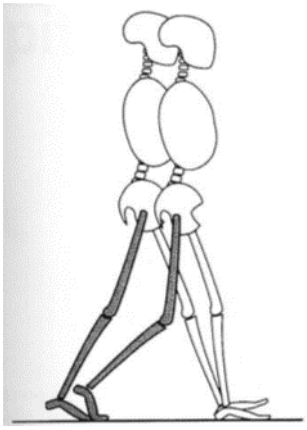

Figure 3.6: Pre swing [31].

- **Initial swing**

  The initial swing phase goes from 62-75% of the gait cycle. During the initial swing, the hip and knee are flexed, and the ankle is partially dorsiflexed to begin advancement of the limb forward and elevation of the foot above the ground. The other limb is in the early mid stance. This first phase accounts for roughly one-third of the swing period. It starts with lifting the foot off the floor and concludes with the swinging foot opposing the stance foot.

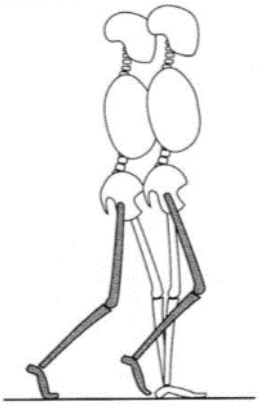

Figure 3.7: Initial swing [31].

- **Mid swing**

  The mid swing phase goes from 75-87% of the gait cycle. During mid swing, further hip flexion allows the limb to move anterior to the body weight line. In response to gravity, the knee is permitted to extend, while the ankle remains dorsiflexed to neutral. The other limb is in the late mid stance. The swing period's second phase begins when the swinging limb is opposite the stance limb. When the swinging limb is forward and the tibia is vertical, the phase is over.

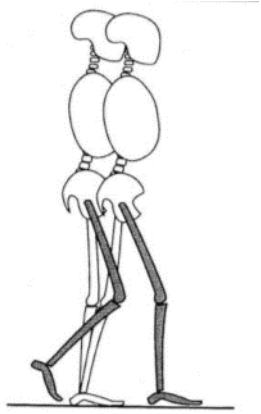

Figure 3.8: Mid swing [31].

- **Terminal swing**

  Terminal swing is the final phase of the gait cycle and goes from 87-100% of the cycle. During terminal swing, knee flexion completes limb advancement, the hip maintains its previous flexion and the ankle remains dorsiflexed to neutral. The other limb is in terminal stance.
  This final phase of the swing starts with a vertical tibia and concludes when the foot hits the floor. The shank moves ahead of the thigh to complete limb progression and the foot is positioned for initial foot contact to start the next gait cycle [31] [32].

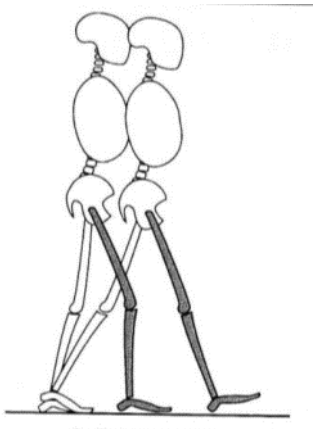

Figure 3.9: Terminal swing [31].

3.2.2 Applications of gait analysis

The majority of the time, gait analysis is performed for clinical studies. In this scenario, the goal is to learn more about a condition affecting a group of patients or the impact of a surgical intervention. Is not used to make clinical decisions for the specific patient. Gait analysis may be conducted to diagnose a pathology (or to differentiate between different disorders), to understand the gravity of the disease (assess its severity or origin), and to forecast the effects of treatment or the lack thereof.
Also, gait analysis can be used to monitor the development of a patient's condition over time, i.e., pre and post operative assessment or to control the evolution of degenerative diseases.

The kinematic and kinetic measures must be able to distinguish between normal and pathological movement patterns as well as between the traits of one disease compared to another. This is only possible if the measurement methods are able to operate with minimal error, therefore, to be sufficiently precise to determine whether a patient's condition is improving, stabilising, or declining. Also, the operators conducting the research must be aware of the characteristics that distinguish healthy walking from disease-impaired walking.

Gait analysis should provide the clinician with information; hence results must often be stated using terminology that clinician can comprehend: the interpretation of data is, in fact, another factor to take into consideration in clinical gait analysis. Therefore, is important that the method used to describe joint kinematic and kinetic is clear, unambiguous, and exhaustive.
Clinical specialists today have a good understanding of normal patterns of movement thanks to the use of well-defined conventions for defining three-dimensional joint kinematics and kinetics. Also, many dysfunctional movement patterns are generally recognised by studying the data and associating specific abnormal patterns to specific pathologies and impairments.

With the use of musculoskeletal modelling, it is also possible to further deepen the movement study. It is possible to add muscles or ligament analysis to the study of kinetic and kinematics. With this it is possible to associate muscle's activation, or the role of ligaments in gait analysis. Not only for a healthy subject but more importantly for patients whose pathology may cause muscle or ligaments deficit.

Lasty, it is important to remember that the study of joint kinematic and kinetic only provides sets of measurements (explain what happens in a specific task during time) but the role played by researchers studying human biomechanics is to link those measurements to a specific action.

3.3 Motion kinematics

3.2.2 Motion capture with skin markers

Traditionally, to evaluate *in vivo* motion kinematics a procedure called *stereophotogrammetry* analysis is used. This technique requires the use of infra-red reflecting markers positioned on specific landmarks of the body. These markers are positioned on the skin and the landmarks are usually bony prominence that are easy to individualize by physicians. They are constructed from a particular material that reflects light in the infrared band.

The main goal of motion kinematic analysis is to reconstruct the trajectories of the markers: this way it is possible to study the patient movement, by following the position of a specific landmark of anatomical segment in the three-dimensional space. To do so it is necessary to specify global and relative reference systems.
The global reference system (or global coordinate frame) is an orthogonal system of axes in solidarity with the laboratory. This way, the position of a point is described by the cartesian coordinates with respect to the global system.
Other than position, when describing the trajectory of anatomical segment, their orientation in space is also needed, since it changes during the motion task analysis. Therefore, a local reference system (or local coordinate frame\body embedded frame), usually attached to the body of interest, needs to be introduced. Three landmarks on the segment must be defined in order to construct a local reference frame and define the three orthonormal axes that compose the system.

When defining the coordinate frames, it is necessary to follow standards imposed by the International Society of Biomechanics (ISB) [34]. The definition of the global coordinate system depends on the type of *calibration* technique that is used (calibration is a technique to assure that the measurements calculated through stereophotogrammetry are accurate) [35]. However, generally, the global coordinate system should be oriented like this: +Y axis upward and parallel to the field of gravity, X is the antero-posterior axis, which coincide with the direction of travel of the subject (anterior direction is considered positive), and Z is the medio-lateral axis (right direction is considered positive). Obviously, all axes are perpendicular to each other.

The local reference system is associated with the task motor subject of the analysis. When building the frames, ISB recommends fixing the origin of the local reference system in the centre of mass of the segment. The axes are defined as: +X axis is anterior, +Y axis is superior, +Z axis is calculated

using the right-hand rule (this way right and left body segments will have +Z axes pointing in different direction: for the left it will point medially, for the right it will point laterally).

As said before, when using stereophotogrammetry analysis, skin markers are needed. These markers are positioned on bony prominence corresponding to specific landmarks. In the stereophotogrammetry laboratories cameras that produce infra-red light are employed. There are typically multiple infra-red cameras in the labs (the least required number of cameras is 12, but the higher the number of cameras, the better is the reconstruction of the movement).
These cameras are able to provide the position coordinate of the markers because they not only emit infrared light but also absorb the light that is reflected by the markers.

ERRORS IN KINEMATICS

In motion analysis instrumental errors are frequently made. The process for obtaining the coordinates of the markers can be inaccurate for a variety of reasons.

Cameras are affected by distortion: this causes the cameras to not receive the correct position of the markers, this leads to measuring an incorrect distance between different markers. This error can be easily prevented by performing *dynamic calibration* (this type of calibration involves a human operator that swings a bar, where markers are attached at a known distance between them, in front of the cameras. This way is possible to calculate a correct factor that will prevent distortion errors).
Flickering phenomenon: it happens when a marker is not seen by at least 2 cameras at the same time. If the marker is not seen by at least 2 cameras, the marker's coordinates can not be recovered.
These two errors are systematic errors and can be easily solved.

Wrong marker placement: the placement of the markers on the anatomical landmarks is carried out by a physician, therefore how well the marker is placed depends on the skill of the operator as well as the constitution of the subject on whom the markers are placed. To minimize this type of error, the marker placement procedure, and relative data acquisition, should be done more than one time:

- By the same physician on the same subject in the same acquisition session (Intra-operator).
- By the same physician on the same subject but in two different acquisition sessions (Inter-session).
- By a different physician on the same subject in the same acquisition session (Inter-operator).

By adopting these measures, it is possible to minimize the inaccurate placement of the markers.

Soft tissue artefact (STA): this error happens because when we place the markers on the skin of the patient, we assume that the marker position is "fixed" (the marker can't move). However, this assumption is far from reality, the markers, due to gravity, muscle forces, elasticity of the soft tissues, are not immobile with respect to the underlying bone: there is sliding of the soft tissue on the bony landmark.

Is important to remember that the procedure of kinematics is subjected to the hypothesis of rigid bodies: this states that the anatomical segments are meant to be rigid, so the relative positions of the landmarks are supposed to remain constant throughout the procedure.

The fact that the markers are not immobile, means that the length between different markers may change during a specific task. So, the hypothesis of rigid bodies is not satisfied.

The artefact error is time-varying and can reach several centimetres in terms of landmark coordinates, and hence several degrees in terms of joint angles. They also have a frequency spectrum that is close to the actual kinematic data, therefore these errors cannot be filtered.

Unfortunately, there isn't a clear solution to overcome this error, but there is a technique to minimize soft tissue artefact. This technique was invented by A. Cappozzo et al. in 1997 [36], and consists in the use of a new set of markers, called *technical markers*, not placed on the bony landmarks.

These markers are arranged on the segments (at least three per segment) so that their position regarding the underlying bone structure does not change, or the changes are negligible, between the static placement and the full dynamic trial.

Using these markers, a technical coordinate system with an origin and three orthogonal axes can be constructed on the segment, according to the rigid body hypothesis.

Then, in order to minimize the SDA error, an algorithm that follows the concept of minimum weighted residual sum squares is applied (this algorithm is based on the Singular Value Decomposition). The principle follows the formula:

$$min \sum_{k=1}^{n} \|e_k\|^2 = min \sum_{k=1}^{n} \|R * p_k + T - l_k\|^2 \quad [37]$$

Where:

- e_k is the elastic energy of the spring-mass system
- p_k represents the coordinates of the technical markers in the technical frame
- l_k represents the coordinates of the technical markers in the global frame
- R is the rotation matrix
- T is the translation matrix

The algorithm determines the R and T matrices that minimise the elastic energy and thus the soft tissue artefact for each frame of the dynamic trial.

Motion capture with skin markers for foot segment

When taking into consideration the foot segment we can see in the picture which landmarks are used.

- The distal apex of the lateral and medial malleoli (indicated with LM and MM respectively).
- The upper ridge of the calcaneus posterior surface (CA).
- The dorsal aspects of the first, second, and fifth metatarsal head (indicated with FM, SM, and VM respectively).

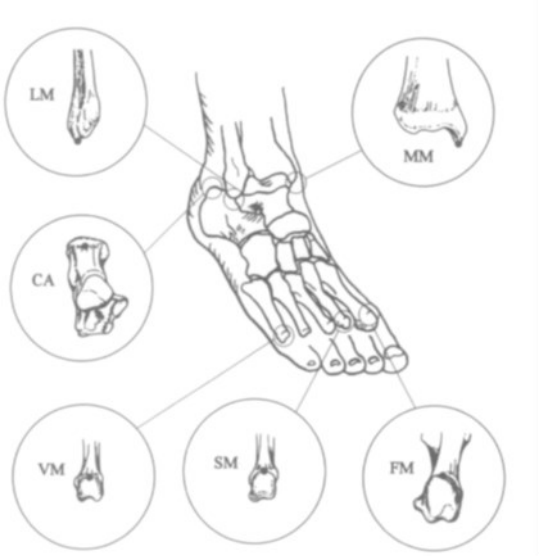

Figure 3.10: Anatomical landmarks in distal tibia and fibula and foot [37].

Founded these, is possible to define bone embedded anatomical frames:

- The origin O_f is located in CA.
- The y_f axis is defined by the intersection of two planes: one defined by FM and VM and the other defined by CA and SM. The y axis positive direction is proximal.
- The x_f axis is orthogonal to the y_f plane and the positive direction is dorsal.
- The z_f axis lies in the quasi-transverse plane and its positive direction is proximal [37].

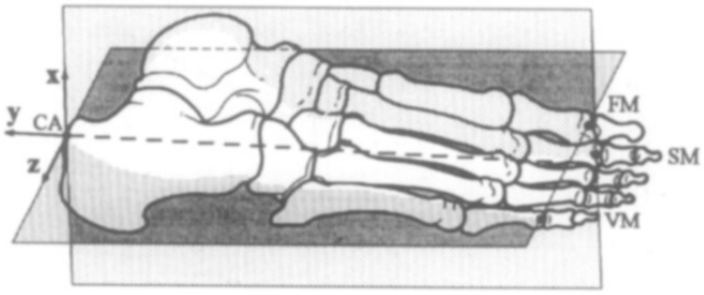

Figure 3.11: Foot bone embedded anatomical frames [37].

Where the markers are positioned on the foot during stereophotogrammetric acquisitions, depends on the protocol that is being followed. A protocol decrees how to acquire the kinematic data from a dynamic movement of a subject. The type of protocol also specifies how many markers can be used and where to position them.

For example, if following the Helen Hayes marker set [38], the number of markers on the foot are three (calcaneus landmark (CA), lateral malleoli (LM), and big toe), while in the Heidelberg Foot Measurement Method [39] the number of markers is higher.

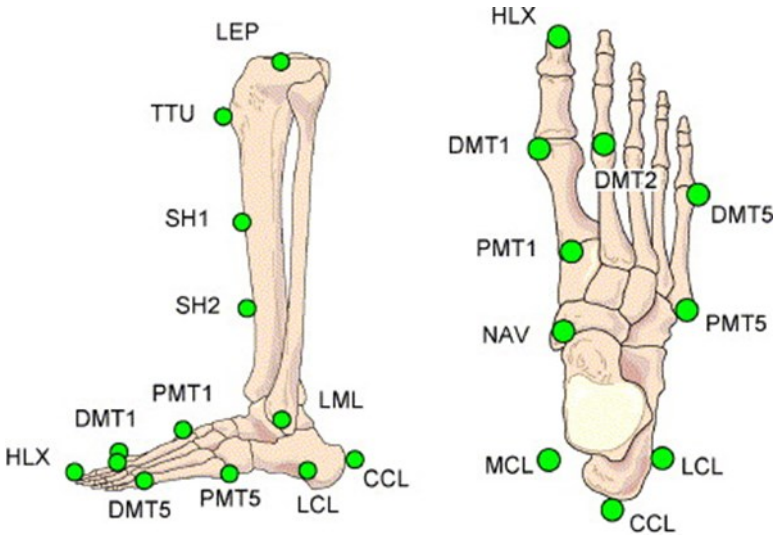

Figure 3.12: Heidelberg foot measurement method - markers placement [39].

Three-dimensional motion capture using skin marker models is a good way to study gait-analysis and calculate joint angles. Even when focusing on patients that have foot-related pathologies, this method is still frequently used. However, there are some drawbacks:

- Skin motion artefacts.
- Because the foot is a highly complex structure, with a high number of bones and joints, many skin marker models oversimplify the kinematic description of the foot. This happens because, rather than measuring the motion of individual bones, many skin marker models monitor the movement of segments that are assumed to be rigid.
- Many bones and joints are not considered in the models as individuals, because they are not accessible for skin markers. For example, skin markers can't access the talus, which position determines hind and midfoot alignment, therefore the ankle joint's movement is determined by the relative movement of tibia and calcaneus.

3.2.3 Medical imaging

Medical imaging is a technique and practice of imaging the interior of a body for clinical examination and medical intervention, as well as visual representation of the activity of some organs or tissues. It aims to expose internal structures.

Computer tomography scan (CT scan) is a type of medical imaging that uses X-ray to obtain detailed images of the body. Focusing on the foot, CT scan allows the visualization of individual foot bone position.

To better study the individual foot bone position during full weight-bearing tasks, it is possible to use a weight-bearing CT scan. By using this type of technology, it is possible to obtain 3D images that are not influenced by projection and/or foot orientation.

As stated in M. Richter [40] study, using a weight-bearing scanning device for 3D imaging acquisition of foot and ankle, allows to measure more accurate bone positions (therefore being able to measure more accurate joint angles) compared to other devices. For example, the use of radiography leads to incorrect angle measurements due to inaccuracies of projection and foot orientation.

However, this technology is limited to static acquisitions, so it's not fitted to evaluate foot bone kinematics. For this reason, the most suitable option is the use of dynamic CT sequences that report bone orientations and locations in the three spatial dimensions over time (4D CT).

Four-dimensional computed tomography allows the recording of numerous pictures over time. These scans can then be played as a video, allowing physiological processes to be examined and internal movements to be tracked.

Different studies had been done to measure foot bone kinematics using this type of technology. In Teixeira et al. [41] study foot kinematics were assessed during pronation\supination and flexion\extension movement controlled by pulling an elastic band to guide motion. This study was performed both in cadaveric specimens and healthy volunteers.

In Buzzatti et al. [42] study a cadaveric foot was subjected to a combined movement of plantarflexion, adduction, and supination in order to study the effect of sectioning the lateral ankle ligaments on the kinematics of the foot. The movement was induced manually through a custom-made wooden device; the device simulated the ankle movement from maximum dorsiflexion to full inversion and back.

However, in both of these experiments, the movement was manually imposed in the 4D CT scanner, therefore not being representative for foot functioning during gait.

Lastly, another study, by H. Boey et al. [2], explored the use of 4D CT in evaluating individual foot bone kinematics during simulated gait. Scanning was combined with an actuated CT-compatible foot manipulator that actively imposes plantar\dorsiflexion and inversion\eversion kinematics by a foot bed.

One of the aims of this study was to validate a protocol on how to impose dynamic foot kinematics representative of the stance phase of gait under weight-bearing 4D CT scanner using a foot manipulator. To do so, seven cadaveric specimens and five healthy volunteers were tested (all with no history of major foot injuries).

During the acquisitions, the participant was positioned in a supine position with the ankle joint lined up with the rotation axis of the foot manipulator and the foot secured to the foot bed. The position of the foot bed was controlled dynamically by three linear actuators, that allows a range of motion (ROM) of 24° in plantar\dorsiflexion (14° plantarflexion and 10° in dorsiflexion) and 11° in inversion\eversion (5.5° each). With this ROM, the stance phase of gait was simulated in 10s.

A full-body harness that the healthy volunteers wore, was utilised to apply force to the foot through a tensioned strap system in the simulation. A specially designed loading apparatus was used to measure cadaveric specimens, as shown in figure 3.13. The loading device is connected to the foot and is made up of two components. One component is fastened to the cadaveric foot's tibia, while the other portion contains a bolt and a spring. The spring is tensioned, and the load is passed from the tibia to the foot by inserting the bolt into the tibial portion.

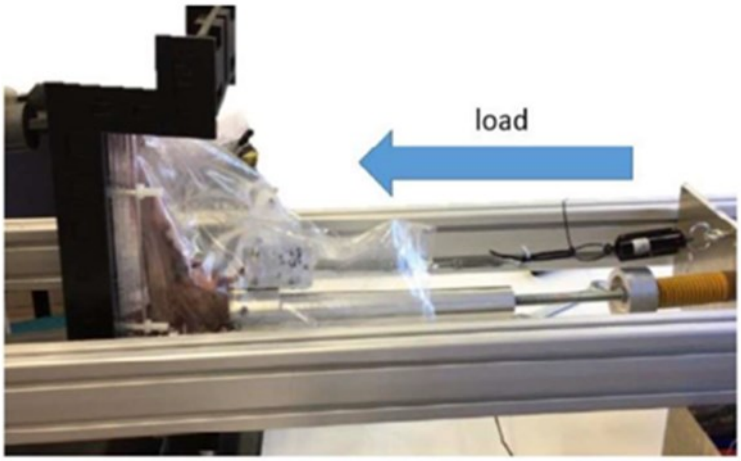

Figure 3.13: Setup used for the cadaveric tests [2].

In the figure 3.14 it is possible to see both a description of the foot manipulator (A), how the foot was positioned during the simulations (B), and the generic kinematics template that was used as the imposed movement in the simulation (C).

Figure 3.14: (A) Description of foot manipulation device; (B) Positioning of the foot in the foot manipulator; (C) generic kinematics input template (solid line: plantar\dorsiflexion, dotted line: inversion\eversion) [2].

Comparing 4D CT to methods that use skin markers to capture foot bone kinematics, it is possible to see that this method has many advantages. In 4D CT scanning:

- There are no skin motion artefacts.
- The position of the talus (useful to determine hind and midfoot alignment) is easily accessible.
- Is possible to calculate the joint angles of each joint individually.
- Using it in combination with a foot manipulation device allows to perform a fast and standardized analysis of the stance phase of gait. This can be very useful for a wide variation of patients (i.e., patients that suffer from talar instability, or that can't successfully perform a traditional gait analysis).

Although this method has many benefits, there are some limitations:

- Because the foot of the participant is attached to the foot bed, is unable to perform heel strike or toe-off, which reduces the amount of plantar/dorsiflexion possible in the ankle joint at the start and finish of stance.
- The stance phase in the study was set at 10s, but in normal conditions it usually lasts about 0.6s.
- The loading applied on the healthy volunteers was not measured.

Chapter 4

4. Materials and methods

The methodologies, modes, and operations used for the modelling aspects of the thesis will be described in this chapter. The data utilized to begin the work, the programmes used, and any necessary revisions and modifications made will all be presented.

4.1 Aim of the project

The goal of this project was to validate a foot musculoskeletal model with the data acquired by Boey et al. [2]. In the study, the data was acquired by using 4D CT in combination with a foot manipulation device on healthy volunteers, CAI patients, and cadaveric specimens. However, only the data from the 11 healthy volunteers was used in this project. The combination of 4D CT and foot manipulator was needed to simulate the stance phase of gait.

Malaquias et al. model was already validated, but only by using motion capture data, which, as it was explained in chapter 3, does not provide specific bony data, while using 4D CT data assures a more accurate validation. Since the extended musculoskeletal model describe the foot biomechanics with higher accuracy compared to other foot models, validating it using detailed data of each joint kinematic is essential.

4.2 Starting point

The final goal of this thesis is to validate an OpenSim musculoskeletal model that allows estimating the foot response when imposing the generic template movement used to move the foot manipulator within the 4D CT setup. This project was developed in the past months from the collaboration between the research group of the bioengineering laboratory of the University of Padova (Italy) and the Human Movement Biomechanics Research Group at KU Leuven (Belgium).

The starting point of the work was the 8 DOF extended foot model created by Malaquias et al. [3]. As explained in chapter 2, this model is able to describe significantly more complex foot dynamic movements, compared to other traditional models available in OpenSim.

The model was further advanced by implementing four contact geometries, to simulate the interaction between the foot and the ground. Since the aim of this project was to recreate the same conditions in the model as in Boey's study, the geometries will simulate the contact between the foot and the foot

manipulator device. They are defined following another study of Malaquias [43]. In the study the contact geometries are defined starting from plantar pressure distributions, where four different ellipsoids were fitted into (Figure 2.5 A). The ellipsoids represent the contact of different regions of the foot: calcaneus, midfoot, forefoot, and toes.

Then, with a three-step approach, visible in the figure 2.5, the contact geometries were created (using a triangular mesh) and later added to the foot model.

The position of the ellipsoids, relative to the foot segments, were estimated using an optimization algorithm.

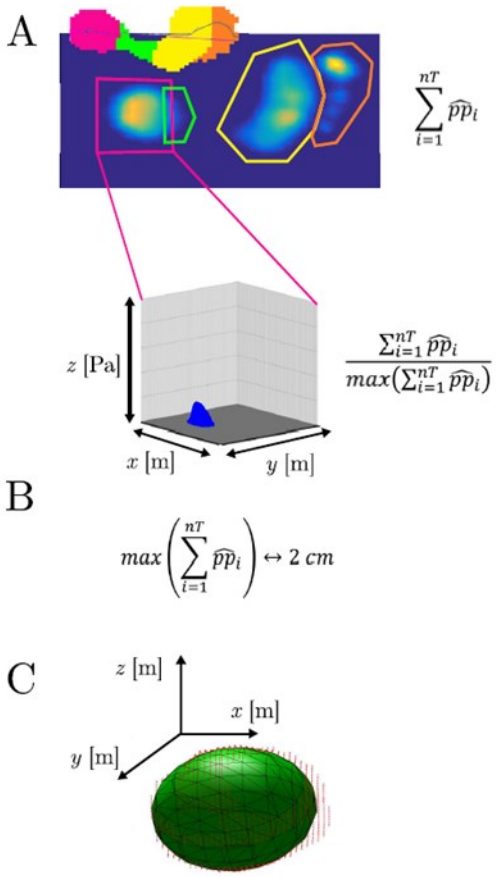

Figure 2.5: Ellipsoid contact geometry computation. (A) Selection of different pressure areas; (B) Conversion of scaled pressures to clouds of virtual points. (C) Ellipsoid fit: least square optimization [43].

The foot manipulator device was incorporated in the model in the form of a plate. The plate is positioned horizontally to the ground and the foot (when in a static position) is placed on top. This assures that the force of gravity is perpendicular to the foot plate.

This positioning of the plate, as can be noticed, is different compared to the orientation it has in Boey's data, where the patient was lying supine, therefore the plate was perpendicular to the ground (at least at the beginning of the experiment). The choice that led to leaving the plate in a horizontal position was for greater convenience while working on the model.

In the figure 4.1 it is possible to see the foot on top of the plate in the OpenSim window.

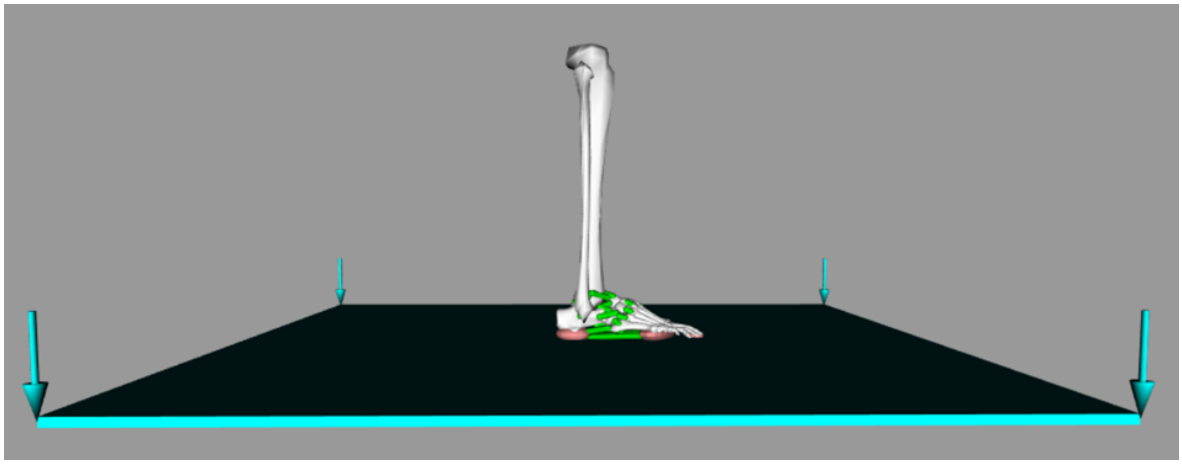

Figure 4.1: Foot and plate model in OpenSim.

The foot model will be the starting point of this work and most of the project will be dedicated to the implementation of it. Only in the end the simulation will be compared with the 4D CT in combination with the foot manipulator device data, to validate the model itself. The methods and the purposes of Boey's study has already been discussed in chapter 3. The data was provided in the form of setting files (i.e., RRA setting file for the imposed plate movement) or MATLAB ((2021b), The MathWorks Inc., Massachusetts) data (i.e., all degrees of freedom movements of the 11 healthy volunteers).

The movement that will be imposed to the plate in the model, is the same kinematic template used to simulate the stance phase of gait in the study. The motion was simulated for 10 seconds: plantar\dorsiflexion (solid line) has a range of motion of 24° (14° plantarflexion, 10° dorsiflexion); inversion\eversion (dotted line) has a range of motion of 11° (5.5° each).

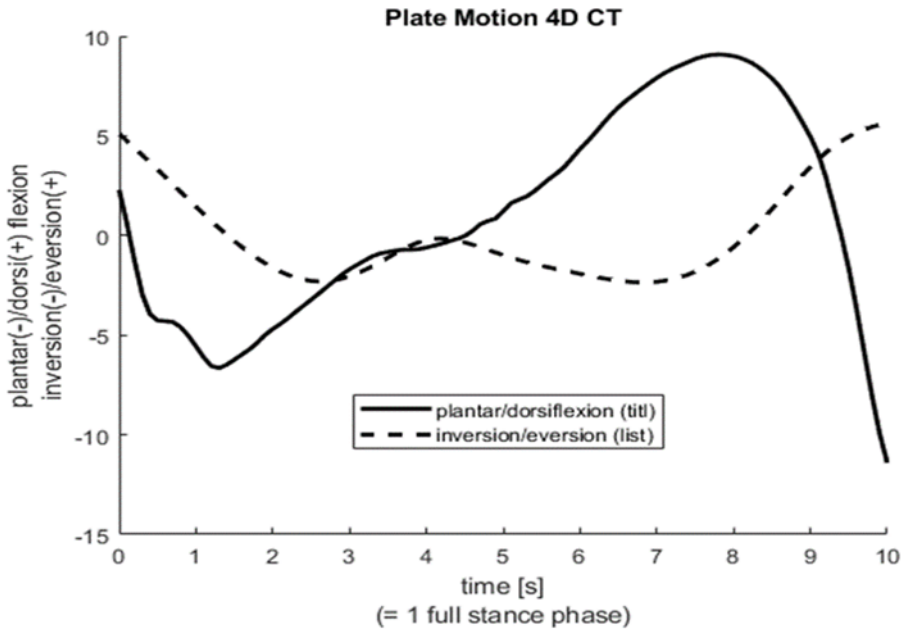

Figure 4.2: Plate motion [2].

The joints in the 4D CT data all are described with 3 DOF, this doesn't correspond with the joint's DOF that the model in the current condition has (in the model every joint only has 1 DOF). Adding degrees of freedom to the model was the first task accomplished.

To summarize the project that will be discussed in this chapter, the following table helps to easily visualize the workflow:

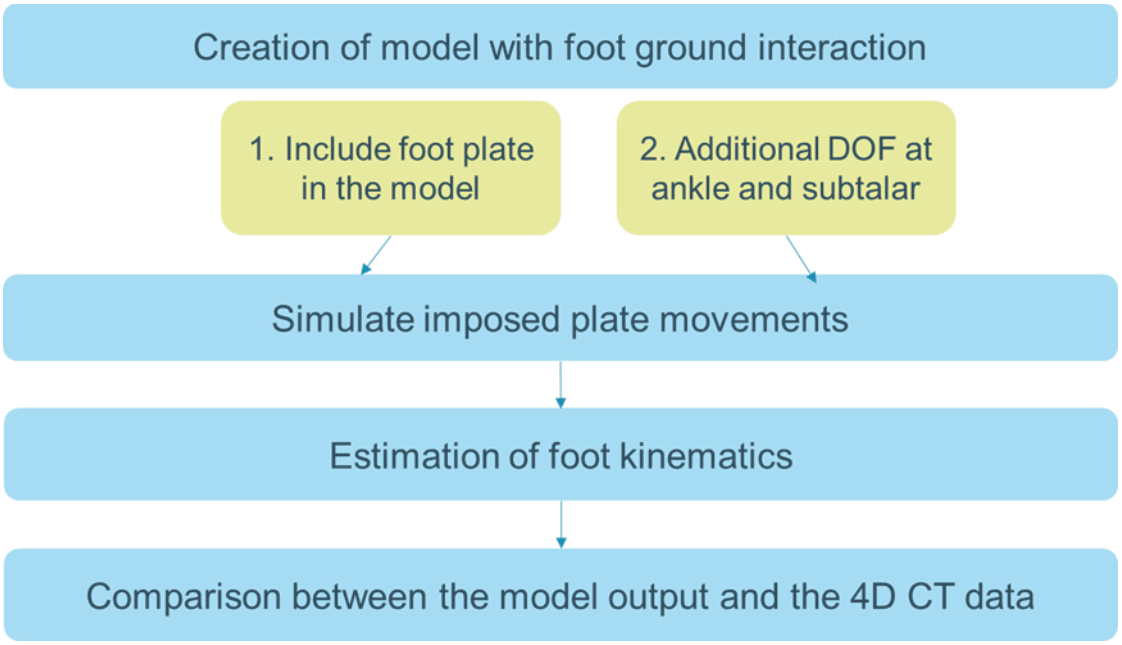

Table 4.1: Workflow of the project.

4.3 Model changes and simulations

This paragraph is dedicated to all the changes made in the model and relative simulations, made to be able to validate the foot model using 4D CT data.

4.3.1 Joints degrees of freedom

Since the 4D CT data's joints are described with 3 degrees of freedom each, while in the extended foot model are described only by 1 DOF, adding DOF at ankle and subtalar joint was needed.
To do so, the degrees of freedom were added directly on the model code on ankle and subtalar joints. The DOF added to the pre-existing one were the 2 rotations (this way the joints can move in plantar\dorsiflexion, inversion\eversion, and internal\external rotation) and 3 translations (following the axis x, y, and z). The translations are not needed but were added for completeness and later locked (so that during the simulations, the joints could not move in those directions).
The maximum range of motion of the 3 rotational DOF is 180° (90° each for plantar\dorsiflexion, 90° each for inversion\eversion and 90° each for internal\external rotation).

Only at ankle and subtalar joints the degrees were added; this decision was made to lighten the computational burden and because these articulations are the ones that respond the most to the imposed movement.

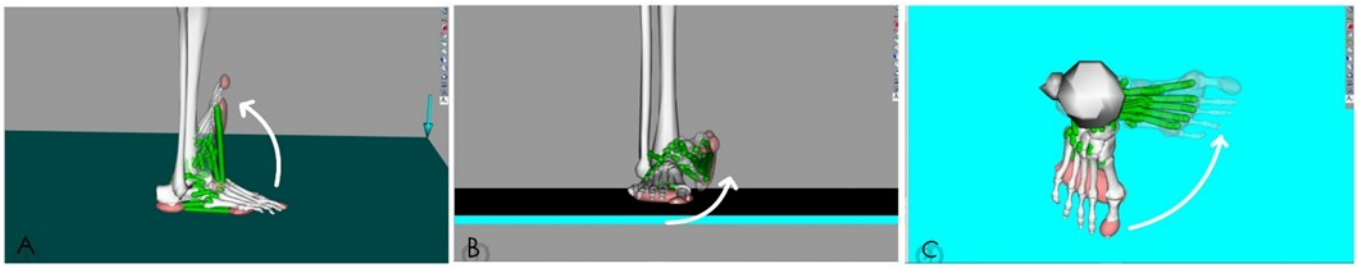

Figure 4.3: Ankle degrees of freedom. The arrow indicates an angle of +90°. (A) plantar\dorsiflexion; (B) inversion\eversion; (C) internal\external rotation.

4.3.2 Contact geometries

The contact geometries were defined as stated in Malaquias's article [43]. The contact geometries are four ellipsoids that are needed to describe the interaction between the foot and the plate. A triangular mech approximates the geometry of each surface and a spring-damper system is placed at the centroid of each triangle of the mesh.

The contact geometries are placed on big toe, forefoot, midfoot, and calcaneus, in correspondence with the most protruding parts of foot's sole.
Since the contact geometries seemed to not match the bony prominence of the foot, they were manually positioned by looking at the plantar pressure of the healthy subject, to have a rough idea on where the contact should be [44].
In the end the contact geometries were positioned as shown in the picture 4.4.

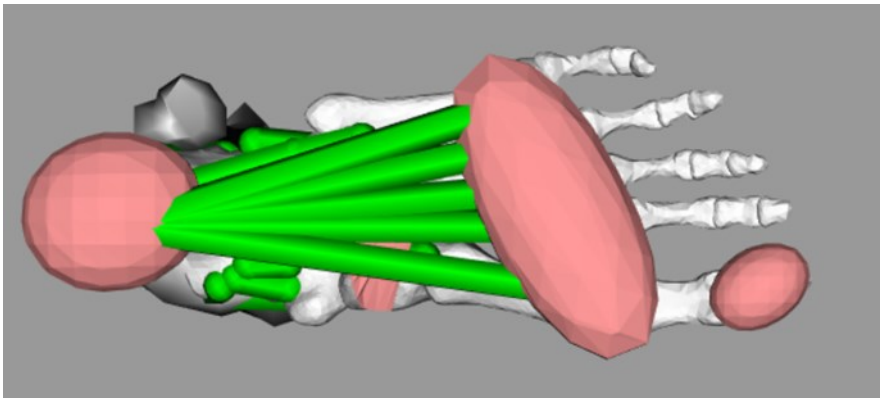

Figure 4.4: Placement of the contact geometries (shown in pink).

4.3.3 Imposed plate movement

To simulate the same conditions of Boey's study, the movement was imposed on the plate. This motion is the generic template that is shown in figure 4.2.

The first thing to do was to run the Residual Reduction Algorithm (RRA). The purpose is to decrease the need for residuals to the absolute minimum that is required to closely follow the specified kinematics.
To run this simulation, the files needed in input were:

- A file containing the imposed plate movement. It's a matrix where the columns are time (goes from 0 to 10 seconds with a step of 0.1), the three degrees of freedom of the plate (the values corresponding to each time step are frame of the imposed plate movement, in this case the internal\external rotation of the plate is zero), and all the DOF of the foot (these are all zeros, because the movement is only at the plate).
- A file that describes the actuators set. It defines the residual and reserve actuators that will be used, as well as their properties such as maximum/minimum force and location.
- A tracking task file that specifies which coordinates to track and the tracking weight.

After running the RRA, it is possible to visualize it on the model. In this case, only the plate is moving while the foot remains motionless.

The output files that are of interest for future analysis are:

- The states file contains the adjusted kinematics and corresponding model states of the simulated motion.
- The controls file that contains actuator excitations.

Lastly, it is possible to portray in a graph the states file, to see if the movement matches Boey's generic template for the foot manipulator. The graph is shown in the picture below and it is possible to note that the plate movement in plantar\dorsiflexion and inversion\eversion are the same as in the experimental setting.

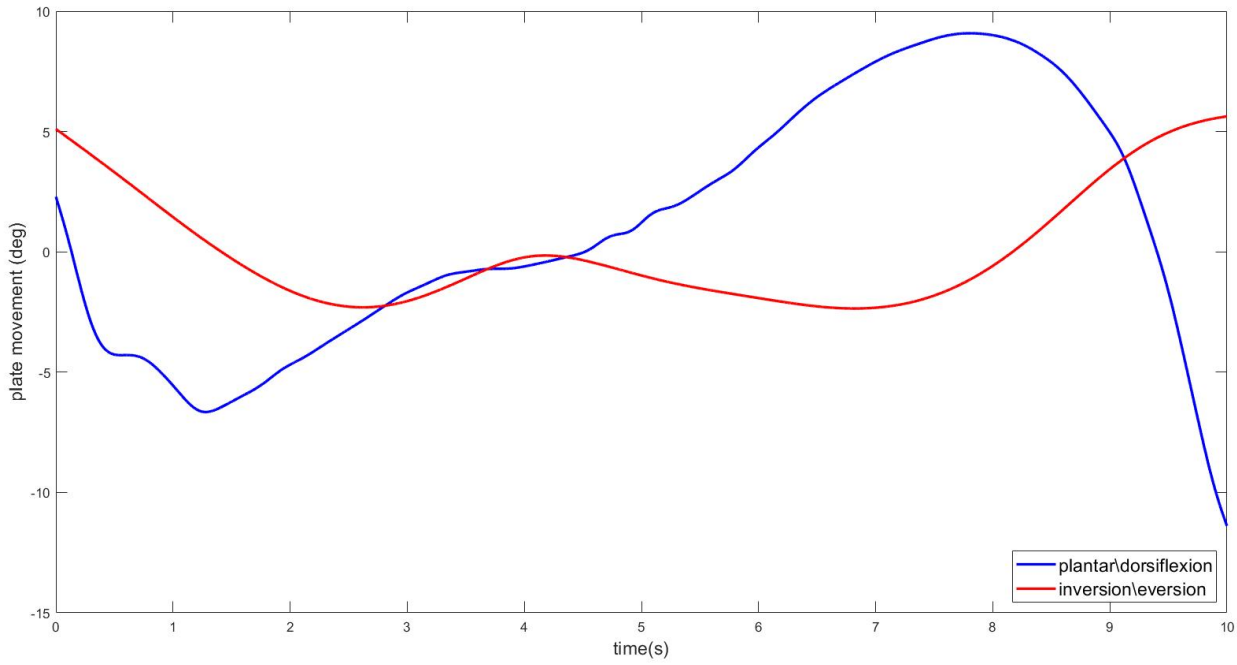

Figure 4.5: Plate movement in plantar\dorsiflexion (in blue) and inversion\eversion (in red).

4.3.4 Forward dynamic simulation

After running the RRA, to simulate the response of the foot model to the plate movement, the Forward dynamic was run.

Forward dynamic can drive a simulation in response to the controls generated by the RRA. In particular, the states and control files described earlier. Other than those, a controls actuator file is needed (already used for the RRA).

At the end of this simulation, what was expected was the foot model following the plate movement so that the output would be comparable to the experimental data. However, in the first simulation the foot would not follow the plate but "bounce" on it and stay in a dorsiflexed position at the end of the simulation (as shown in figure 4.6).

Being this completely different from what was expected, the next thing to do was to find what was causing the foot to move this way.

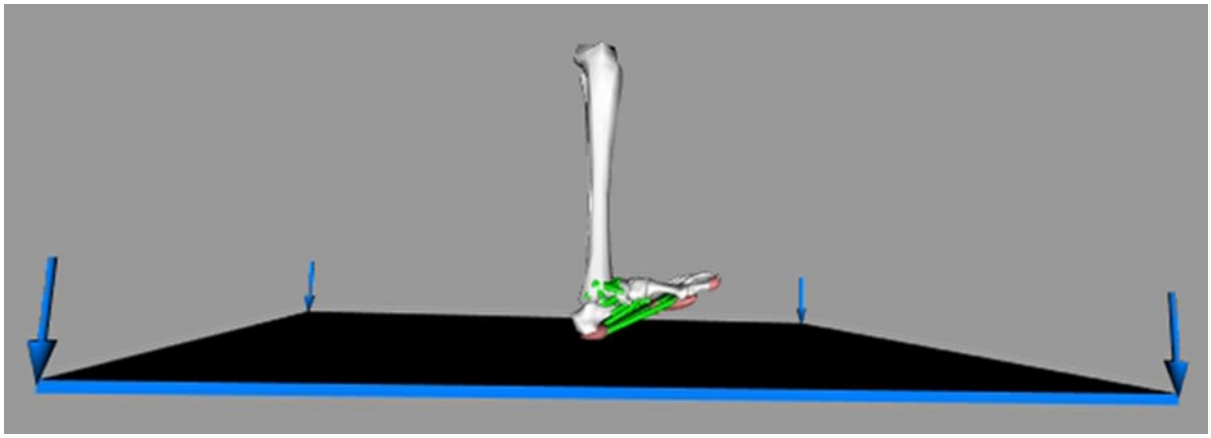

Figure 4.6: Last frame of the Forward Dynamic simulation. It is possible to see the foot in a dorsiflexed position, while it should be in contact with the plate.

4.3.5 Trial and error process

Since the forward simulation did not run as expected, finding what was causing the problem was needed. However, not knowing exactly what was causing it, led to a sequence of attempts to understand the situation. This, unfortunately, ended up being the bigger challenge of the project.

First, seeing that the foot was bouncing on top of the plate, completely not following the plate movement, led me to think that the issue lied in the contact geometries. For this reason, the values that characterized the contact geometries were investigated.

- Changing the stiffness of contact geometries: in the initial model, the stiffness of all contact geometries was set at 100000. By changing it the behaviour of the foot changed: if the value was increased, up to 10000000, the foot would bounce at a higher frequency (still not following the plate movement) while if it was decreased, till 1000, the foot would still bounce but with a lower rate. By lowering the stiffness value, the foot would also sink into the foot plate. Also, the foot would still stay in dorsiflexion at the end of the simulation.
  So, changing the stiffness only did what was expected, that is, make the contact geometries more or less flexible. Meaning that this value was not responsible for the foot not following the plate.
  Eventually, the foot stiffness was set at 1000000.

- Changing the friction coefficients of the contact geometries: in the initial model the values were 0.8 for static and dynamic friction and 0.5 for viscous friction. These values were

changed in decimals (i.e., 0.08, 8, 80). Increased static or viscous friction would lead to a decrease in bouncing amplitude, while the opposite happened for dynamic friction.
In any case the foot would still not follow the plate and not stay in contact in the end.
These values, like the stiffness, are not responsible for the foot not following the plate.
Eventually, the values were left as in the initial model.

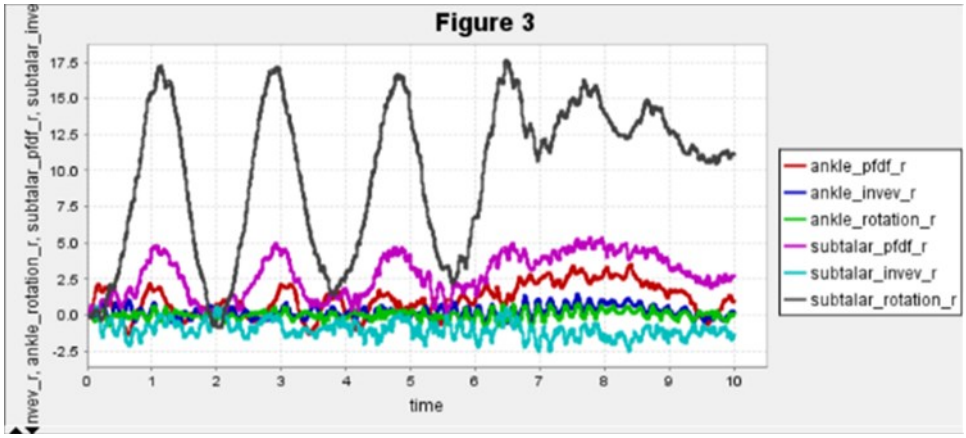

Figure 4.7: Ankle and subtalar movement in plantar\dorsiflexion, inversion\eversion, and inter\external rotation. In this simulation stiffness was 100000, static and dynamic friction was 0.8 and viscous friction was 0.5.
Is possible to see the swinging trend of the curve, caused by bouncing and vibrating of the foot on top of the plate.

Seeing that the contact geometries were not responsible for the foot model not behaving as expected, the next thing to check was the definition of the foot plate itself.
This ended up being responsible for the bouncy behaviour of the foot model; because with a new definition of the plate the foot remained more in contact during the simulation and did not display a spring-like behaviour. However, this didn't make the model act as wished: the foot would still maintain a dorsiflexed position at the end of the simulation and not follow the imposed movement of the plate.

This led to trying other approaches in order to overcome the incorrect foot movement. First, two seconds were added at the beginning of the simulation. During this time the plate would just stay still and only after the 2 seconds passed, the imposed movement would begin. This assured that the foot model had a "loading" time before the start of the imposed movement.

Then, the values describing the gains for position and velocity errors (named kp and kv respectively) were investigated.

These values define the behaviour of the error dynamics and can be written in terms of system poles. For a stable critically damped system (real negative poles), $kp = \lambda^2$ and $kv = -2\lambda$. The coefficients in the initial model were set to kp = 100 and kv = 20.

Changing these parameters led to the discovery that the accuracy of the plate movement (how well the plate followed the imposed kinematic template) depended on these values. For higher values (i.e., kp = 100, 1000) the footplate would better follow the template, but the foot response was worse (for too high values the foot was barely moving). For lower values the plate movement would still follow the template, but with less range of motion, the foot actions, however, were better (the foot had a less stiff behaviour and was more responding to the plate movement). Lastly, a simulation without kp and kv was conducted and here the plate movement had an oscillating trend that didn't follow the template. However, this was the first simulation done where the foot would follow the plate movement for the whole duration of the simulation (except for the last instant, where the foot would remain in a dorsiflexed position, but with a less accentuated angle). In the figures 4.8 and 4.9, it is possible to see the plate movement in the simulation where kp and kv values were omitted (red line), in the simulation with kp and kv values (green line), and the correct template (blue line). It can be easily spotted that the red line has an oscillating trend, very different from the other two curves.

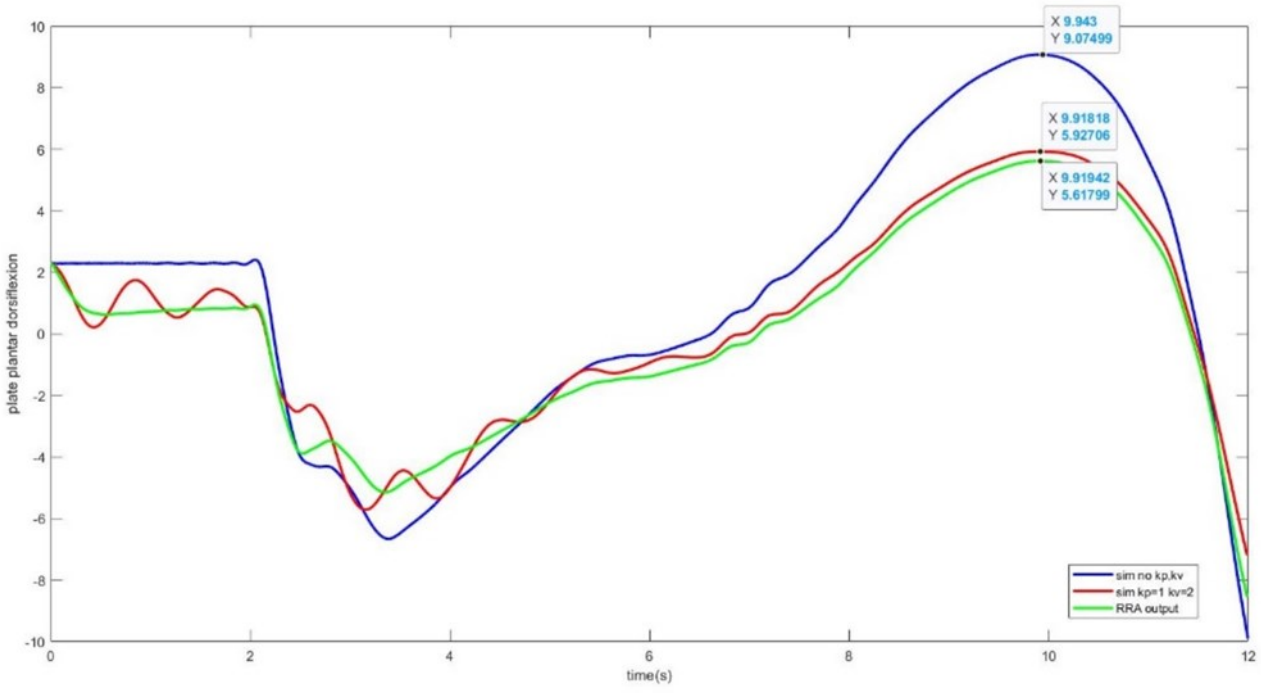

Figure 4.8: Comparison between the plate movement in plantar\dorsiflexion of imposed plate movement (blue), plate movement of the simulation with kp=1 and kv=2 (green), and plate movement of the simulation without kp and kv values.

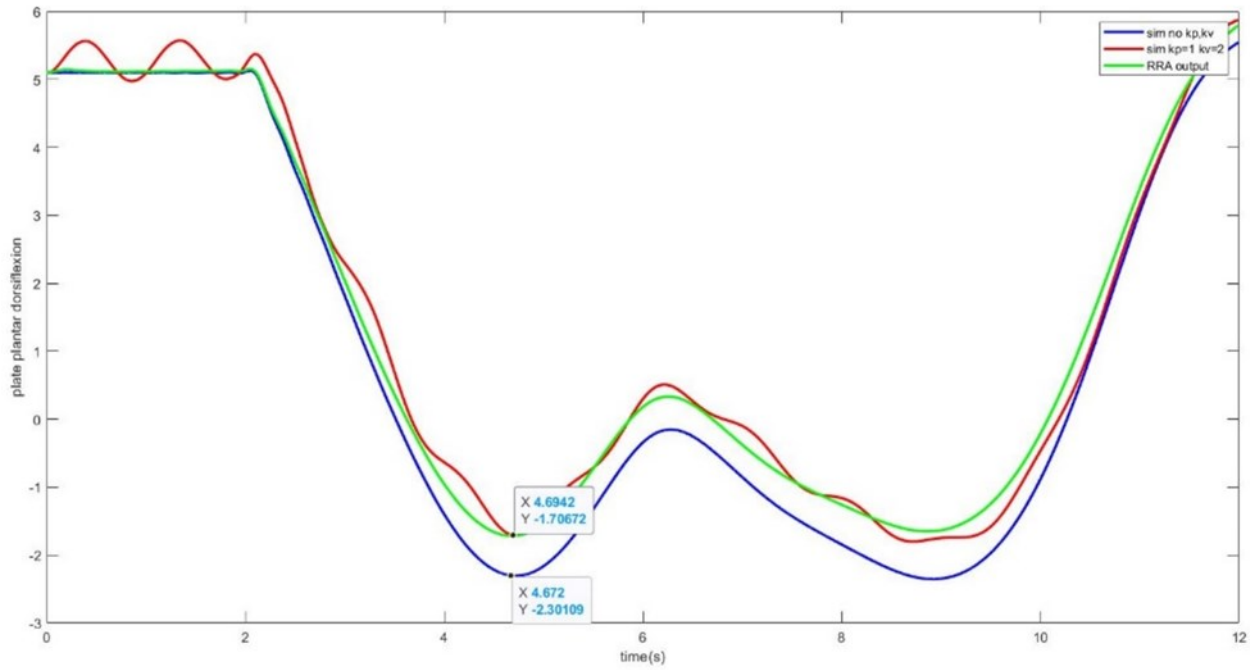

Figure 4.9: Comparison between the plate movement in inversion\eversion of imposed plate movement (blue), plate movement of the simulation with kp=1 and kv=2 (green), and plate movement of the simulation without kp and kv values.

This led to the decision that the best option was to find a middle ground between the accuracy of plate movement and a foot model that responded to the plate moving. For this reason, in the final model the values were set at 1 for kp and 2 for kv.

To understand why the foot would not stay in contact, the ligaments forces were checked. First by changing the ligaments forces defined in the model. This, as expected, only changed the stiffness of the foot movement, without altering the movement trend of the foot.
After that, were inspected the forces produced by the ligaments in output, to understand if the ligaments were causing higher forces that caused the foot's behaviour. With a custom-made MATLAB code, the ligament forces of different simulations (i.e., with kp and kv values defined in the model or without) were compared. This showed that the forces produced were not higher than a few Newtons, therefore could not be responsible for the foot behaviour at the end of the simulation.

After inspecting the differences that changing all these values would make on the model movement, there wasn't much more that could be changed. However, it was known that in Boey's study both volunteers and CAI patients, while subjected to the 4D CT exam, wore a full-body harness to mimic the body weight. Unfortunately, the magnitude of load was not measured [2].
To mimic this condition, load was added to the foot segments. The wight was added in different ways:

- 10kg added only at the tibia. When the weight is only added to the tibia the foot barely moves during the simulation.
- 10kg distributed on foot segments (3kg on calcaneus, 2kg on midfoot, 3kg on forefoot, and 2kg on toes). When the weight is distributed as described the foot stays in contact during the whole simulation. However, the weight pushes the plate in a plantarflexed position in the beginning of the simulation, resulting in a plate movement that doesn't follow the template.
- Other two simulations were made with 6kg and 2.5kg distributed on foot segments (2kg on calcaneus and forefoot, 1kg on midfoot and toes, for the first simulation; 1kg on calcaneus, 0.5kg on midfoot, forefoot and toes, for the second). These simulations are not much different than the one with 10kg distributed, the only difference is that the degree of plantarflexion of the plate is lower.

In the picture 4.10 it is possible to see the comparison between the plate movement template (in blue) and the plate movement for the simulation with 10kg distributed (in green). Only the plantar\dorsiflexion movement is shown because the inversion\eversion had not been altered by the weight.

In the first two seconds, where the plate should be still, there is a big movement in plantarflexion. Then, at 2 seconds of time the imposed movement starts, but the plate is now in a crooked position, meaning that the movement is now compromised. This caused a big difference in dorsiflexion: the difference between the template and the simulation's output is approximately 8°.

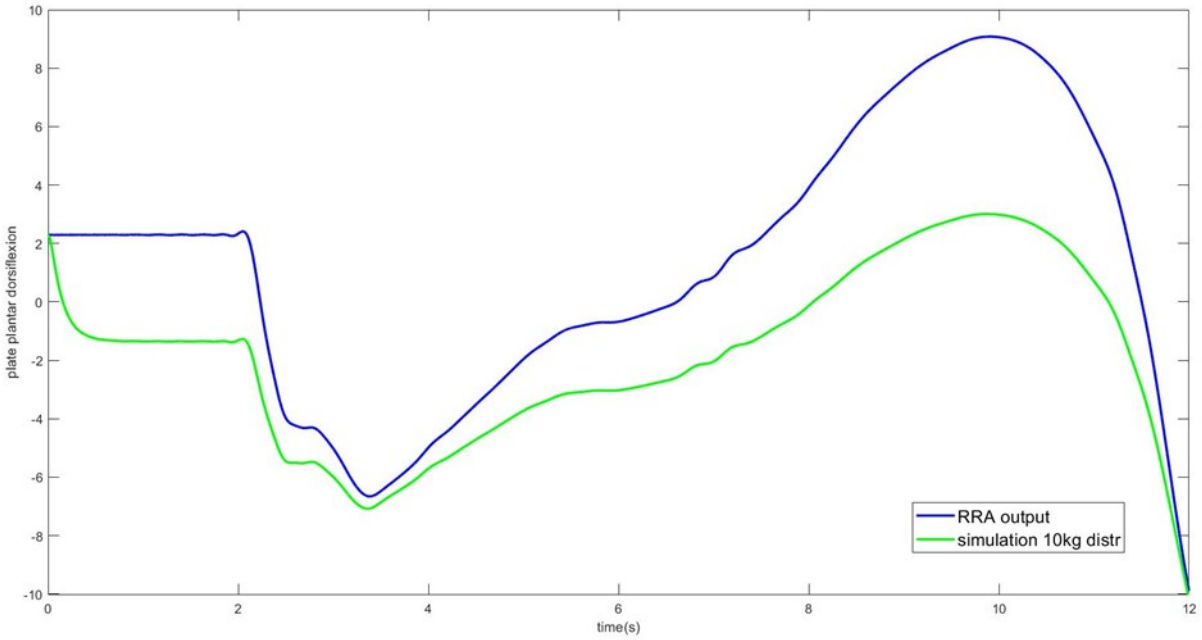

Figure 4.10: Plantar\dorsiflexion movement of the plate. The curve in blue is the imposed template, the curve in green is the plate movement for a model with 10kg added on the foot segments.

Adding weights in the foot segments assured that the plate would stay in contact, but the imposed movement was not accurate. For this reason, the last thing to try to make the foot stay in contact was to add *bushing forces*. A bushing force is the force proportional to the deviation of two frames. To block the foot model in contact with the plate, corresponding bodies of foot (i.e., 3D points on the outer layer of contact geometries) and plate were coupled in the bushing force description. The bushing force is proportional, if the two corresponding points were to translate from one another, the force would increase, making it more difficult for the points to depart from one another. To keep these bodies aligned, it generates a passive force.

It is possible to think of the bushing forces as being composed of 3 linear and 3 rotational spring-dampers, which act along or about the bushing frames [45].

To define the bushing force on the model three parameters are needed:

- The location of the first body. In the case described, the force needs to help the foot model to stay in contact with the plate, so the first body needs to be one of the contact geometries. To define the location, a point was chosen on the outer layer of the contact geometry and their coordinates reported in the bushing force code.
- The location of the second body. The second body needs to be the plate; the coordinates that will be used are the ones that correspond to the first body's coordinate (but on footplate this time).
- The translational stiffness of the force. The higher this value the higher will be the force that keeps the two bodies together.

In the first attempt, the bushing forces were applied on calcaneus and forefoot contact geometries. This arrangement however resulted in the foot not staying in contact with the plate but assuming a dorsiflexed position throughout the simulation.

Because the calcaneus was always in contact in almost every simulation that was made, the bushing force on that contact geometry was removed and instead applied on the toe.

Therefore, the bushing force was applied on the forefoot and big toe contact geometries. This tactic assured a simulation where the foot stayed in contact for the whole duration of the simulation (even in the last frame) with a plate movement that was relatively good.

Different values for translational stiffness were used (e.g., 5000, 15000, 50000). By using higher stiffness, the foot movement would better follow the imposed movement. Regarding the plate, its movement was not really affected by the change in stiffness. The "best" simulation was the one with a stiffness of 50000.

In the pictures 4.11 it is possible to see the last frame of the simulation. Compared to other simulations where the foot would stay in a dorsiflexed position (as shown in figure 4.6), here the foot is clearly still in contact by the end of the trial.

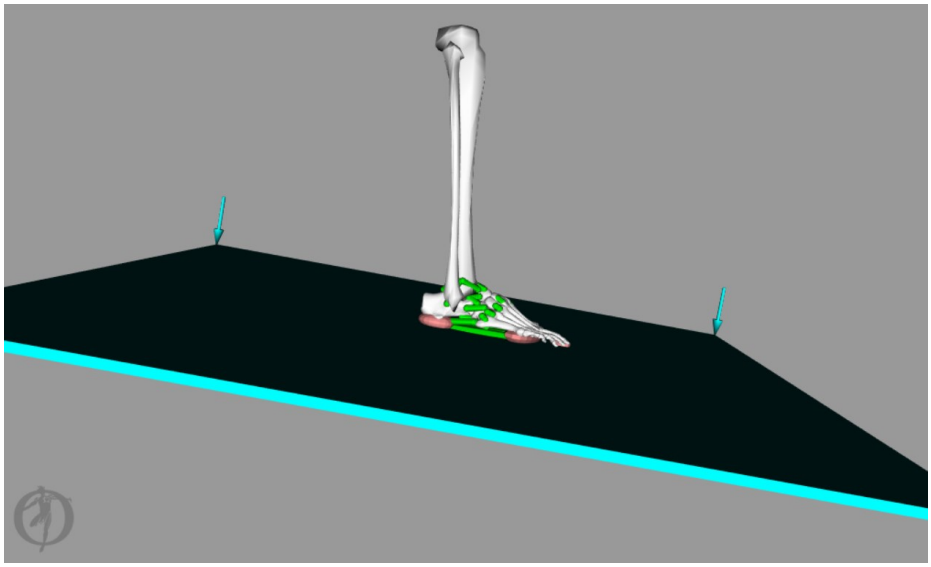

Figure 4.10: Last frame of the simulation with bushing force on forefoot and toe. Upper figure: lateral vision; lower figure: frontal vision.

Chapter 5

5. Results

The following chapter presents the results obtained with the forward simulation analysis.
In the previous chapter, all the modifications that were made on the model to make it follow the imposed plate movement were explained. In both the simulation with the load added on the foot segments and the simulation with the bushing forces, the foot model followed the plate movement. So, the best simulation was obtained by merging these features together. In particular, 2.5kg (distributed 1kg on calcaneus, 0.5kg on midfoot, forefoot and toes) were added on the foot segments and bushing force was imposed on forefoot and toes.
When performing the forward dynamic simulation, the foot would stay in contact with the plate, following the imposed movement. It is now possible to compare the movement of the DOF of ankle and subtalar with the experimental data acquired by Boey et al [2].

5.1 Plate movement

The following graphs represent the comparison between the original plate kinematic template (in blue) with the plate movement in the simulation with added load and bushing force.

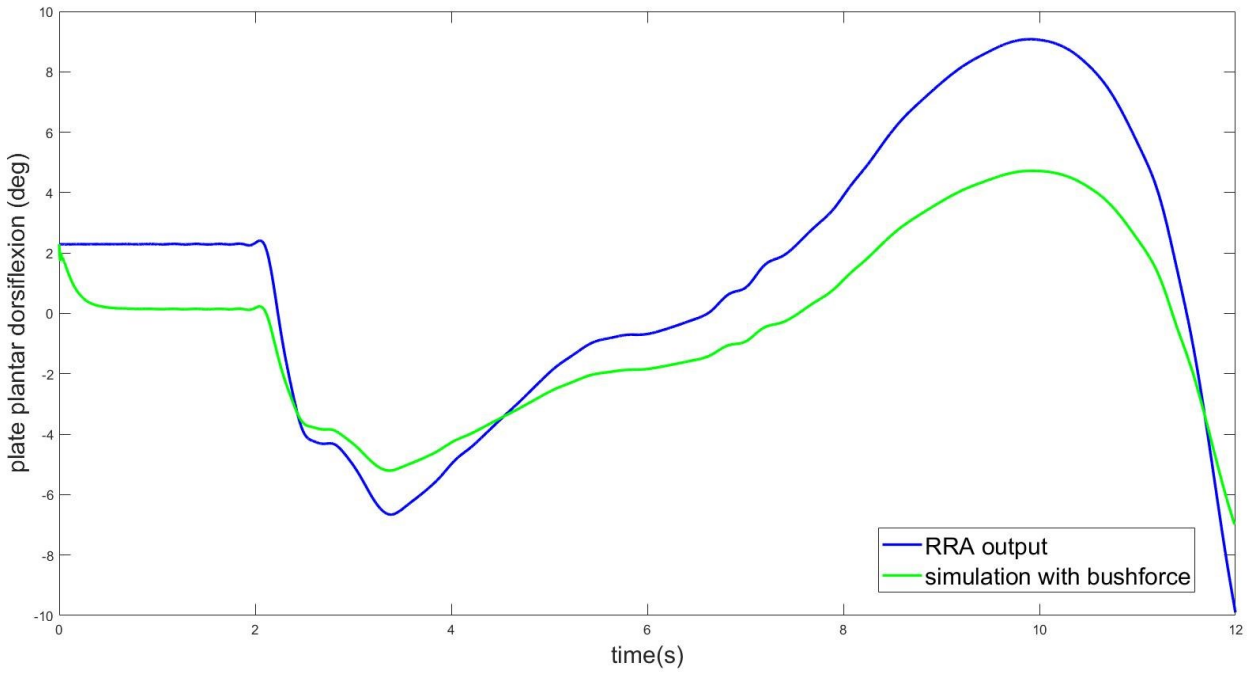

Figure 5.1: Plantar\dorsiflexion plate movement.

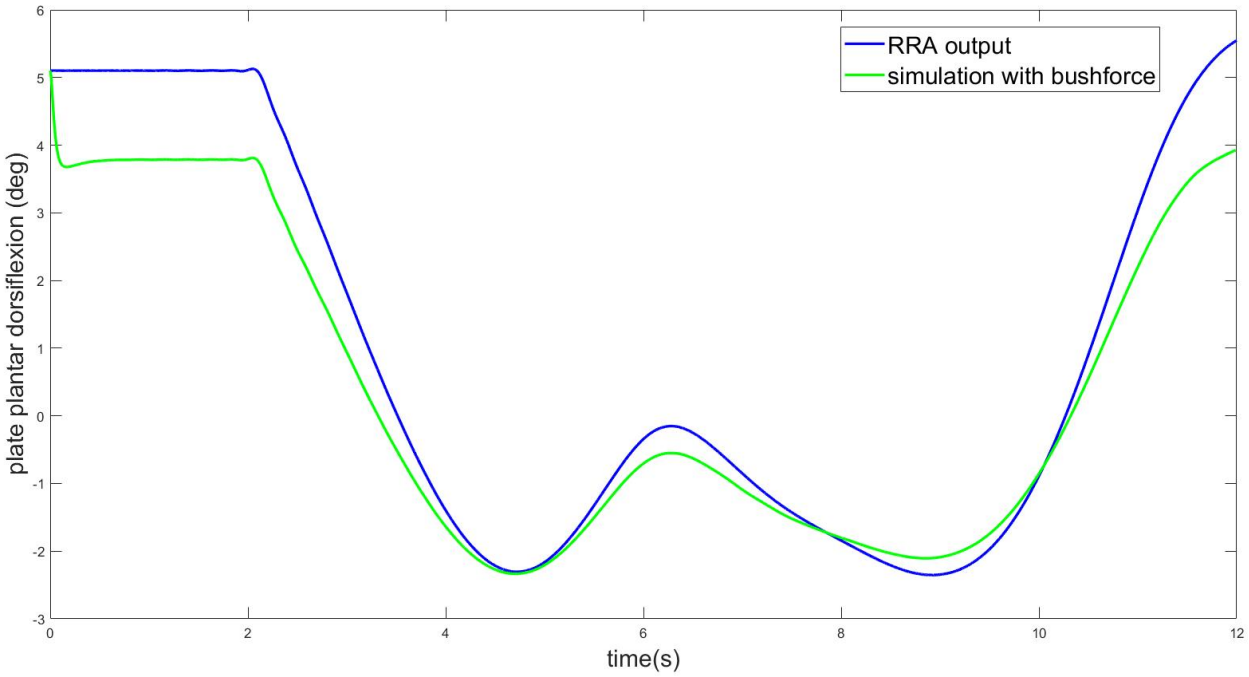

Figure 5.2: Inversion\eversion plate movement.

	Original kinematic template	Model output
Plantar\dorsiflexion	20.5°	11.6°
Inversion\eversion	8.0°	6.3°

Table 5.1 Plate range of motion.

5.2 Ankle Degrees of Freedom

In the following graphs are the comparisons between the experimental data (acquired by Boey et al. [2]) and the simulation outputs of the ankle joint's DOF (plantar\dorsiflexion, inversion\eversion, and internal\external rotation). The experimental data were plotted in the form of average and standard deviation data, of the movement of the 11 healthy subjects.

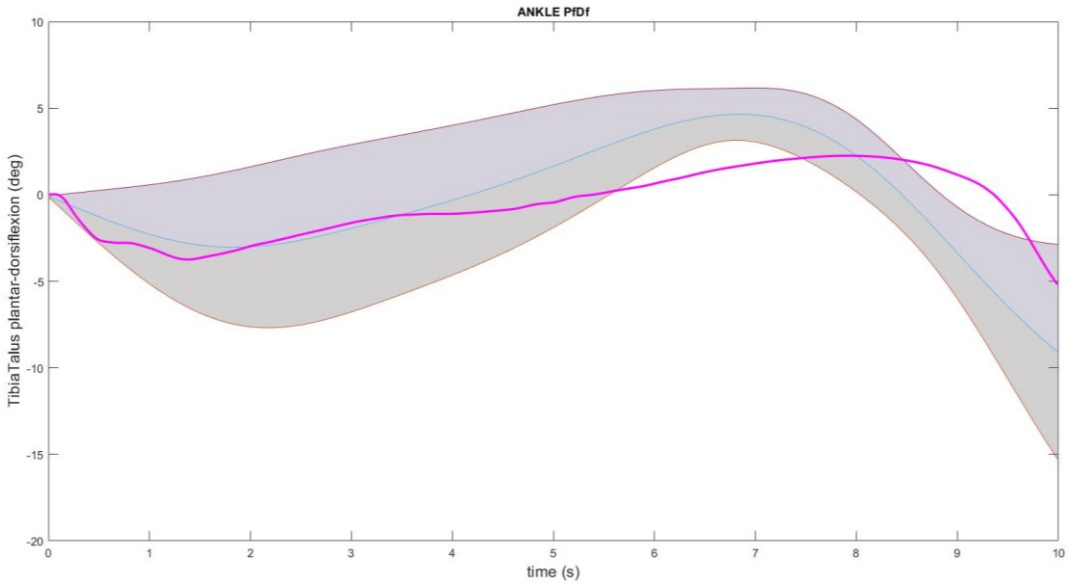

Figure 5.3: Ankle plantar\dorsiflexion. OpenSim output is in pink, experimental data is in grey.

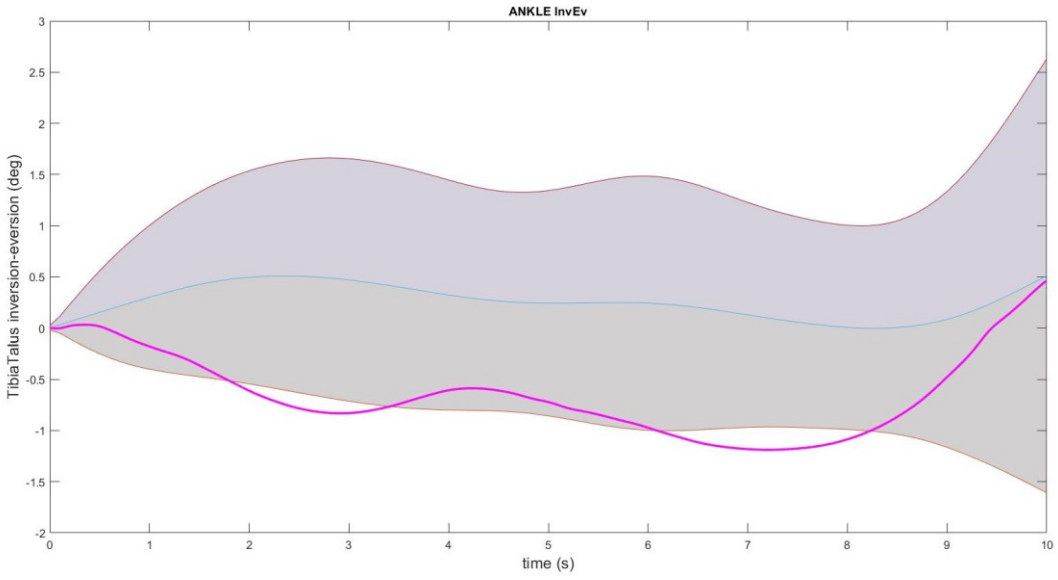

Figure 5.4: Ankle inversion\eversion. OpenSim output is in pink, experimental data is in grey.

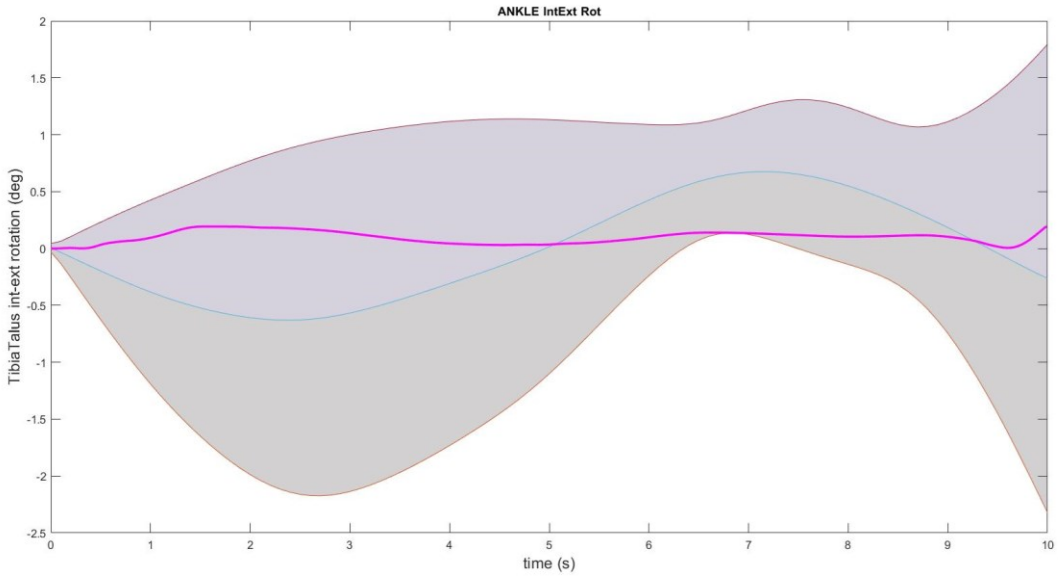

Figure 5.5: Ankle internal\external rotation. OpenSim output is in pink, experimental data is in grey.

	4D CT data (deg)	Model output (deg)
Plantar\dorsiflexion	17.12 ± 3.30	7.36 ± 0.01
Inversion\eversion	2.43 ± 1.47	1.63 ± 0.01
Internal\external rotation	2.86 ± 1.09	0.19 ± 0.01

Table 5.2 Ankle range of motion.

5.3 Subtalar Degrees of Freedom

In the following graphs are the comparisons between the experimental data (acquired by Boey et al. [2]) and the simulation outputs of the subtalar joint's DOF (plantar\dorsiflexion, inversion\eversion, and internal\external rotation).

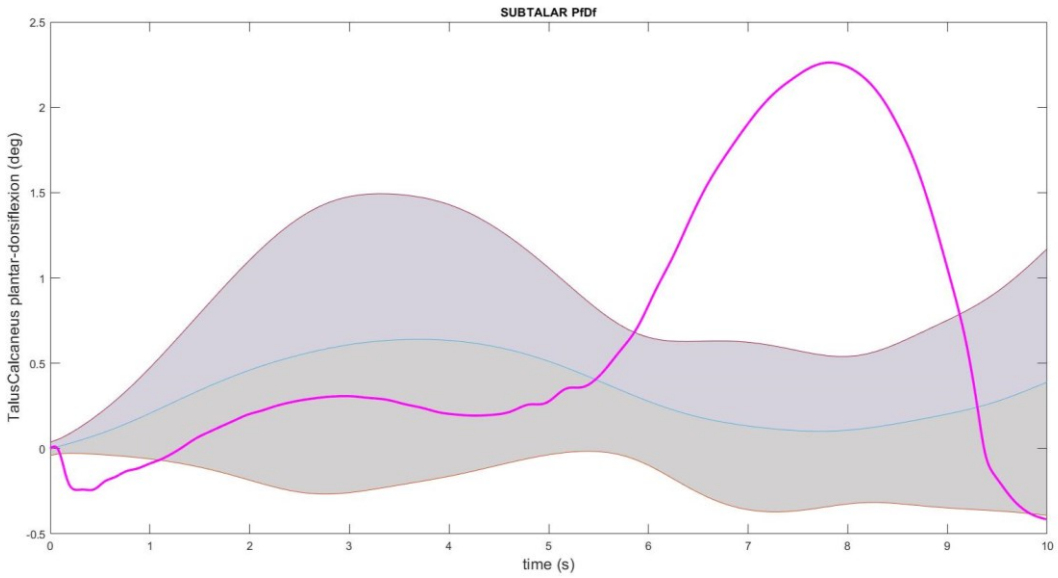

Figure 5.6: Subtalar plantar\dorsiflexion. OpenSim output is in pink, experimental data is in grey.

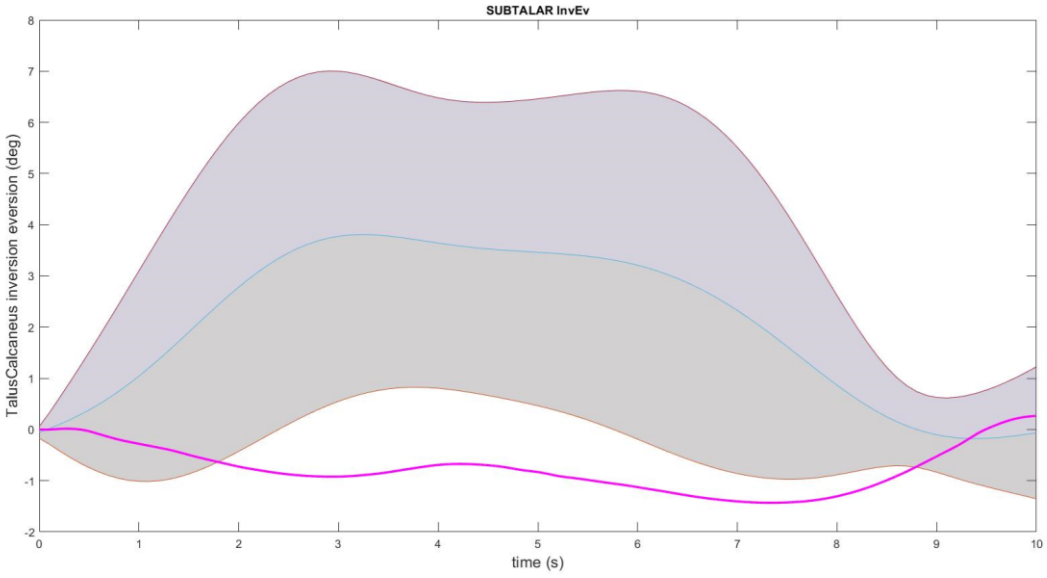

Figure 5.7: Subtalar inversion\eversion. OpenSim output is in pink, experimental data is in grey.

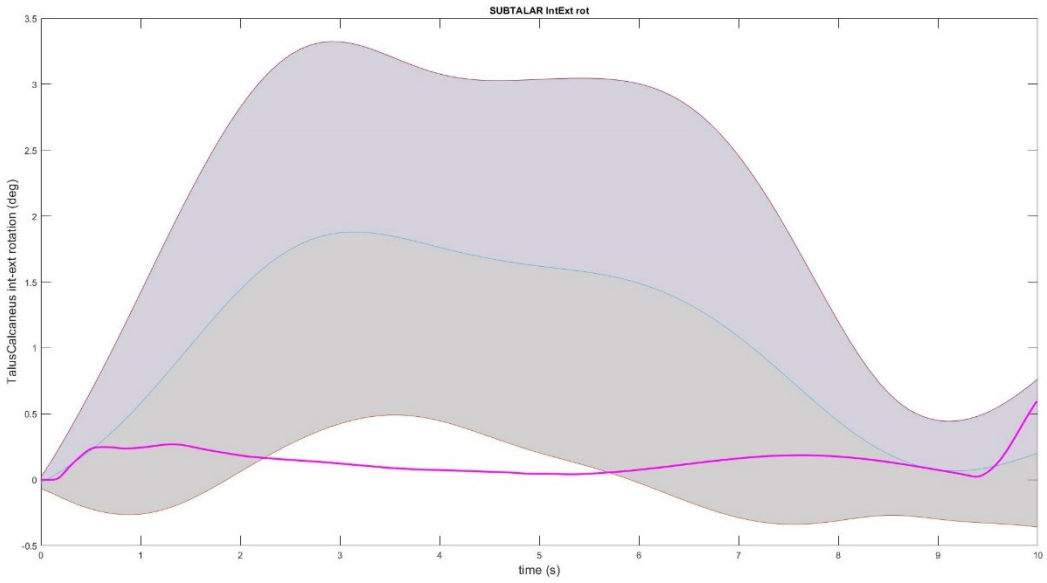

Figure 5.8: Subtalar internal\external rotation. OpenSim output is in pink, experimental data is in grey

	4D CT data (deg)	Model output (deg)
Plantar\dorsiflexion	1.30 ± 1.08	2.68 ± 0.01
Inversion\eversion	5.86 ± 3.18	1.70 ± 0.01
Internal\external rotation	2.63 ± 1.40	0.60 ± 0.01

Table 5.3 Subtalar range of motion.

Chapter 6

6. Discussion and conclusion

The goal of this project was to validate an extended foot musculoskeletal model [3] based on in vivo 4D CT data acquired in combination with a foot manipulation device to simulate the stance phase of gait. The data used to validate the model were of the 11 healthy volunteers of the study [2].
Working on the foot musculoskeletal model, the output wanted was to simulate the same conditions of the study. If this was successful, the model would be validated and could be used in the future to simulate other data acquired through the same method.

In the material and methods chapter, were explained all the modifications that were made to the extended 8 DOF foot model originally developed by Malaquias et al. [3]. The same circumstances of the study needed to be simulated, therefore the first two modifications made to the model were to add the foot manipulator (in the form of a plate) and increase the degrees of freedom of the ankle and subtalar joints. Later, the forward simulation was run. However, the model didn't respond as expected to the imposed plate movement, so different trial simulations were made. In the following simulations, the major problem was that the foot would not maintain contact with the plate; either by bouncing on top of it, or by staying in a dorsiflexed position at the end of the trial. Also, in some simulations, even when the foot would follow the plantar\dorsiflexion movement of the plate, the foot would fail to follow the inversion\eversion movement.
Since the plate was positioned horizontally to the ground, and the gravity force was defined in the model, it was expected that the foot would stay in contact with the plate (helped by the force of gravity). However, this was not the case and led to further investigation of specific model components such as the contact geometries and the ligaments.
Contact geometries were the first to be examined, being the ones that should impose the interaction between the foot and the ground. The values that were changed were stiffness and friction (viscous, static and dynamic). However, changing the values that define the contact geometry did not help to make the foot stay in contact. In fact, stiffness only acted on the rigidity of the contact geometries, making the foot sink into the plate if the coefficient was too low (<10000).
Seeing that in most of the simulations the foot would maintain a dorsiflexed position right in the end, it was thought that the ligaments may be the cause. Thinking that they might be producing high forces that would compromise the model movement. But checking the forces did not reveal any that was higher than a few newtons, meaning that the ligaments were not responsible for the foot staying up.

Another issue was that the foot plate movement would not perfectly match the imposed motion in most of these simulations, compromising the whole movement. The gains for position and velocity errors (kp and kv) were then investigated. Changing these variables showed that the higher they were the best the plate movement was following the imposed one, but at the expense of the foot, that was then barely moving. Therefore, to have a simulation where the foot would have a decent response, we had to compromise on the plate perfectly following the template.

Among the trial variations of the model, adding load on the foot segments and adding bushing forces were the most successful. Therefore, a model with 2.5kg distributed on the foot segments (1kg on calcaneus, 0.5kg on midfoot, forefoot and toes) was simulated with the Forward Dynamic tool adding bushing forces on the forefoot and toes contact geometries, with a translational stiffness of 50000. The load was added to simulate the weight that was added on the cadaveric specimens in Boey's study [2]. After some trials, where different loads were added on the foot, it was set to 2.5kg because higher masses would compromise the plate movement. For the bushing force stiffness, different values were tested, and 50000 was fixed because it made the foot stay in contact. This simulation was the best out of all the other simulations made, since the foot would maintain contact with the plate both in plantar\dorsiflexion and inversion\eversion.

From the output of the tool, the movement of the plate, ankle, and subtalar were extrapolated. These were then compared with the data acquired using the 4D CT setup. The graphs with the comparison are shown in the results chapter.

Regarding the plate movements, it is possible to see that both plantar\dorsiflexion and inversion\eversion follow the same trend of the imposed kinematic. However, the range of motion (RoM) is visibly lower; this can be seen especially for plantar\dorsiflexion, where there is almost 9° of difference between the model output and the data. For inversion\eversion the difference is not as big, and the peak difference is visible mostly in the beginning and end of the simulation (the difference is almost 2°).

The fact that the plate range of motion is much lower than the original kinematic template, may explain the fact that the RoM of the joints are also lower than the experimental data. However, as it is possible to see in the graphs of ankle and subtalar DOF, the model outputs not only have lower RoM, but also very different trends compared to the experimental data.

Only the ankle plantar\dorsiflexion has a trend that is similar to the 4D CT data, even if the two curves do not match. In both the experiment and the model this DOF is the one with the higher RoM.

The others DOFs of the ankle are very different compared to the data, and for internal\external rotation the RoM is almost zero.

When considering the subtalar, neither of the model curves match the experimental data. Plantar\dorsiflexion is the only DOF that has a higher RoM, but if confronted with the data, inversion\eversion should be the higher.
Even if this was the only simulation where the foot stayed in contact throughout the entire simulation, the joints movements showed that this simulation cannot be compared to the 4D CT data.

After all the changes that were made and investigations on the description of the model, it was concluded that the cause of the malfunction could not rest in the model itself. Rather, the reason behind the impossibility of running a simulation where the foot would actively follow the plate (without being constrained by bushing forces), could be caused by the approach made to validate the model.
It is important to highlight that in this work the 3.3 version of OpenSim was used. The extended musculoskeletal model was developed using this version, therefore was chosen to develop this project. However, in new releases of the software, i.e., the 4.4 version, new features have been implemented [46]. For example, it is possible to use functions that allow for better tracking of the imposed movement by minimizing or constraining a model output at the end of the simulation, such as '*MocoOutputTrakingGoal*'. Also, was implemented an option, '*MocoCasADiSolver*' that allows to enforce model constraints in interval midpoints, to fix situations where, during a simulation, path constraints would not be always enforced [46].
These changes might help push the model to follow the imposed plate movement, so that when running the forward simulation, the plate movement would not be compromised, as well as prevent the foot from portraying undesired movements.

In conclusion, because the output does not match with the 4D CT data, the model could not be validated with the data provided. The work done made it possible to understand what changes may or may not help to obtain the desired simulation, but has failed to fulfil its initial goal, implying that more work on the subject needs to be done.
Hence, to validate Malaquias et al. [3] model, a possible solution might be to take advantage of the new functions that OpenSim offers, to ensure simulations where the model movements are comparable to the 4D CT data.

References

[1] M. S. J. R. S. D. A. Seth, "OpenSim: a musculoskeletal modeling and simulation framework for in silico investigations and exchange," *Procedia IUTAM,* pp. 212-232, 2011.

[2] T. M. T. N. S. C. S. V. M. W. C. J. V. S. I. J. Hannelore Boey, "Validation of 4D CT scanning in combination with a foot manipulator device to evaluate individual foot bone kinematics during simulated gait in chronic ankle instability patients," *The American Journal of Sports Medicine,* 2020.

[3] C. S. W. A. F. D. G. G. D. J. V. S. a. I. J. Tiago M. Malaquias, "Extended foot-ankle musculoskeletal models for application in movement analysis," *Computer Methods in Biomechanics and Biomedical Engineering,* 2016.

[4] R. B. R. D. M. Solomonow, "EMG-force relations of a single skeletal muscle acting across a joint: dependence on joint angle," *J. Electromyogr. Kinesiol.,* pp. 58-67, 1991.

[5] M. d. Z. M. S. A. a. J. R. Morten Enemark Lund, "On validation of multibody musculoskeletal models," *Journal of engineering in medicine,* no. 226, pp. 82-94, 2011.

[6] J. H. T. U. A. H. C. D. e. a. A. Seth, "OpenSim: Simulating musculoskeletal dynamics and neuromuscular control to study human and animal movement," 2018.

[7] J. D. Edward J.C. Dawe, "Anatomy and biomechanics of the foot and ankle," *Orthopedics and Trauma,* pp. 279-286, August 2011.

[8] R. Abbound, "Relevant foot biomechanics," *Current Orthopedics,* pp. 165-179, 2002.

[9] "Tendon vs. Ligament," National Library of Medicine, [Online]. Available: https://medlineplus.gov/ency/imagepages/19089.htm.

[10] C. O'Leary, "Joints and ligaments of the foot," 30 June 2022. [Online]. Available: https://www.kenhub.com/en/library/anatomy/joints-and-ligaments-of-the-foot.

[11] "Pain in Ball of Foot," 2018. [Online]. Available: https://www.braceability.com/blogs/info/ball-of-foot-pain.

[12] A. R. C.W. Chan, "Foot biomechanics during walking and running," *Mayo Clin Proc,* pp. 448-461, 1994.

[13] M. Andersen, "Introduction to musculoskeletal modelling," *Computational Modelling of Biomechanics and Biotribology in the Muscuosckeletal System,* pp. 41-80, 2021.

[14] R. B. R. D. M. Solomonow, "EMG-force relations of a single skeletal muscle acting across a joint: dependence on joint angle," *Journal of Electromyography and Kinesiology,* pp. 58-67, 1991.

[15] S. B. E. K. e. a. J.A. Martin, "Gauging force by tapping tendons," *Nature Communications,* 2018.

[16] S. Poelert, E. Valstar, H. Weinans and A. A. Zadpoor, "Patient-specific finfite element modeling of bones.," *Journal of engineering in medicine,* pp. 464-478, 2013.

[17] R. B. H. G. M. G. P. Tomas A.Correa, "Accuracy of generic musculoskeletal models in predicting the functional roles of muscles in human gait," *Journal of Biomechanics,* vol. 44, pp. 2096-2105, 2011.

[18] Z. S. I. J. B. K. A. C. L. Santinon, *Personalization of generic musculoskeletal model in OpenSim,* 2022.

[19] "Scaling," Opensim documentation, [Online]. Available: https://simtk-confluence.stanford.edu:8443/display/OpenSim/Scaling.

[20] C. A. E. G. C. J. J. R. S. D. Samuel Hamner, "OpenSim Tutorial #3 Scaling, Inverse Kinematics, and Inverse Dynamics".

[21] "Inverse kinematics," [Online]. Available: https://simtk-confluence.stanford.edu:8443/display/OpenSim/Inverse+Kinematics.

[22] "Getting started with inverse dynamics," [Online]. Available: https://simtk-confluence.stanford.edu:8443/display/OpenSim/Getting+Started+with+Inverse+Dynamics.

[23] "How RRA works," Opensim Documentation, [Online]. Available: https://simtk-confluence.stanford.edu:8443/display/OpenSim/How+RRA+Works.

[24] "Getting started with RRA," [Online]. Available: https://simtk-confluence.stanford.edu:8443/display/OpenSim/Getting+Started+with+RRA.

[25] "Getting started with Forward Dynamics," [Online]. Available: https://simtk-confluence.stanford.edu:8443/display/OpenSim/Getting+Started+with+Forward+Dynamics.

[26] "How to use the Forward Dynamics Tool," [Online]. Available: https://simtk-confluence.stanford.edu:8443/display/OpenSim/How+to+Use+the+Forward+Dynamics+Tool.

[27] C. Au, "Gait 2392 and 2354 Models," 2012. [Online]. Available: https://simtk-confluence.stanford.edu:8443/display/OpenSim24/Gait+2392+and+2354+Models.

[28] A. G. T. M. F. S. e. a. A. Scarton, "A methodological framework for detecting ulcers' risk in diabetic foot subjects by combining gait analysis, a new musculoskeletal foot model and a foot finite element model," *Gait & Posture,* vol. 60, pp. 279-285, 2018.

[29] J. Hicks, "The mechanics of the foot I – the joints," *J Anat.,* no. 87, pp. 345-357, 1953.

[30] M. E. L. C. S. C. G. O. a. J. R. Mark de Zee, "Validation of musculoskeletal models: the importance of trend validations," 2010.

[31] V. S. Y. J. S. D. Ashutosh Kharb, "A review of gait cycle and its parameters," *International Journal of Computational Engineering & Management,* vol. 13, 2011.

[32] ProtoKinetics, "Understanding phases of the gait cycle," 2018. [Online]. Available: https://www.protokinetics.com/understanding-phases-of-the-gait-cycle/#:~:text=The%20gait%20cycle%20can%20be,foot%20is%20in%20the%20air..

[33] T. &. J. R. &. B. M. &. S. R. &. B. R. &. M.-M. A. Stöckel, "The mental representation of the human gait in young and older adults.," *Frontiers in Psychology,* 2015.

[34] F. C. v. d. H. H. (. V. M. M. P. V. R. C. A. J. N. A. R. K. e. a. Ge Wu, "ISB recommendation on definitions of joint coordinate system of various joints for the reporting of human joint motion—part I: ankle, hip, and spine," *Journal of Biomechanics,* vol. 35, pp. 543-548, 2022.

[35] A. C. G. V. A. C. Valentina Camomilla, "An optimized protocol for hip joint centre determination using the functional method," *Jurnal of Biomechanics,* pp. 1096-1106, 2005.

[36] A. C. U. D. C. a. F. P. Aurelio Cappozzo, “Surface-Marker Cluster Design Criteria for 3-D Bone Movement Reconstruction,” *IEEE Translactions on biomedical engineering,* vol. 44, 1997.

[37] F. C. U. D. C. A. L. A Cappozzo, “Position and orientation in space of bones during movement: anatomical frame definition and determination,” *Clinical Biomechanics,* vol. 10, no. 4, pp. 171-178, 1995.

[38] H. K. R. E. W. M. P. Kadaba, “Measurement of lower extremity kinematics during level walking,” *Journal of Orthopedics Research,* vol. 8, pp. 383-392, 1990.

[39] L. A. D. H. S. J.Simon, “The Heidelberg foot measurement method: Development, description and assessment,” *Gait & Posture,* vol. 22, pp. 411-424, 2006.

[40] B. S. S. Z. S. H. MartinusRichter, “PedCAT for 3D-imaging in standing position allows for more accurate bone position (angle) measurement than radiographs or CT,” *Foot and Ankle Surgery,* vol. 20, pp. 201-207, 2014.

[41] A.-S. F. A. J. G. L. I. L. M. P. A. B. Pedro Augusto Gondim Teixeira, “Quantitative Analysis of Subtalar Joint Motion With 4D CT: Proof of Concept With Cadaveric and Healthy Subject Evaluation,” *American Journal of Roentgenology,* vol. 208, pp. 150-158, 2017.

[42] B. K. J. A. T. S. J.-P. B. G. V. G. e. a. Luca Buzzatti, “Four-dimensional CT as a valid approach to detect and quantify kinematic changes after selective ankle ligament sectioning,” *Scientific Reports,* 2019.

[43] W. A. F. D. G. I. J. J. V. S. Tiago M. Malaquias, “PLANTAR PRESSURE BASED ESTIMATES OF FOOT KINEMATICS DURING GAIT – A LEAST SQUARES OPTIMIZATION APPROACH,” 2018.

[44] C. V. Scheidt, “Modelling and Optimization of Prosthetic Feet and Design of a Passive Printable Prosthetic,” 2019.

[45] A. Seth, “OpenSim::BushingForce Class Reference,” [Online]. Available: https://simtk.org/api_docs/opensim/api_docs/classOpenSim_1_1BushingForce.html#details.

[46] “What's new in OpenSim 4.4?,” [Online]. Available: https://simtk-confluence.stanford.edu:8443/pages/viewpage.action?pageId=83468789.

[47] J. R. M. T. M. Cronskär, “Combined finite element and multibody musculoskeletal investigation of a fractured clavicle with reconstruction plate,” *Computer methods in Biomechanics and Biomedical Engineering,* pp. 740-748, 2015.

[48] M. K. A. B. B. Hintermann, “Peritalar Instability,” *Foot and Ankle Int.,* vol. 33, pp. 450-454, 2012.